Nanochannels Preparation and Application in Biosensing

Alfredo de la Escosura-Muñiz[†] and Arben Merkoçi[†,‡,*]

[†]Nanobioelectronics & Biosensors Group, CIN2 (ICN-CSIC), Catalan Institute of Nanotechnology, Campus UAB, Bellaterra (Barcelona), Spain and
[‡]ICREA, Barcelona, Spain

ABSTRACT Selective transport in nanochannels (protein-based ion channels) is already used in living systems for electrical signaling in nerves and muscles, and this natural behavior is being approached for the application of biomimetic nanochannels in biosensors. On the basis of this principle, single nanochannels and nanochannel arrays seem to bring new advantages for biosensor development and applications. The purpose of this review is to provide a general comprehensive and critical overview on the latest trends in the development of nanochannel-based biosensing systems. A detailed description and discussion of representative and recent works covering the main nanochannel fabrication techniques, nanoporous material characterizations, and especially their application in both electrochemical and optical sensing systems is given. The state-of-the-art of the developed technology may open the way to new advances in the integration of nanochannels with (bio)molecules and synthetic receptors for the development of novel biodetection systems that can be extended to many other applications with interest for clinical analysis, safety, and security as well as environmental and other industrial studies and applications.

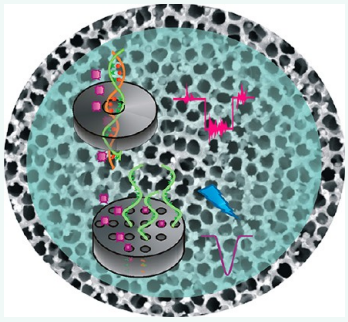

KEYWORDS: nanochannels · nanopores · biosensing · protein sensing · DNA sensing · stochastic sensing · solid-state ion channel · optical sensing · electrochemical sensing

Development and application of biosensing systems is one of the leading sectors of state-of-the-art nanoscience and nanotechnology. Biosensing systems are under commercial development for numerous applications that include the detection of pathogens, the measurement of clinical parameters, the monitoring of environmental pollutants, and other industrial and sensing and security uses. The most effective way of providing biosensing systems to potential customers, especially those with limited budgets, might be to modify the technology so that it can run on everyday equipment, rather than on specialized apparatuses.[1,2] In this context, the use of nanomaterials is proving to be advantageous not only in the design of bioanalytical systems but also in the improvement of existing biodetection systems.[3−7]

Nowadays, there is an increasing interest in measuring and investigating transport and electrochemical phenomena in membrane samples that contain a single pore of nanoscopic diameter. Selective transport in nanochannels (protein-based ion channels) is used in living systems for electrical signaling in nerves and muscles. This natural behavior is being approached for the application of nanochannels in biosensors. Nanoporous materials also show a dramatic increase in surface/volume ratio that enhances the signals corresponding to interaction between solutes and surfaces including biomolecule reactions. On the basis of this principle, nanochannel arrays and single nanochannels seem to present promising new features for biosensor development.

The fundament of sensing using nanochannels is based on the concept of the Coulter counter, a device patented in 1953 by Wallace Coulter[8,9] that consists of two chambers containing an electrolyte solution and separated by one or few more microchannels. When a microscopic particle enters through the microchannel, a change in the electrical conductance is detected. This resistance change can be recorded as electric current or voltage pulse, which can be correlated to size, mobility, surface charge, and concentration of the particles. Due to its simplicity, this device has been used in hospitals for the determination of white and red blood cells and also in the industry of paint, glass, ceramics, and food manufacture. The Coulter counter was designed to measure particles in the micrometric scale, but for biosensing purposes, devices able to detect molecules in the nanometric scale are needed and for this reason the research in this field is focused in the last years on the development of channels of nanometric size[10−12] inspired by the natural ion channels and able to detect molecules such as proteins, DNA strands, *etc.* (Figure 1A).

* Address correspondence to arben.merkoci@icn.cat.

Received for review March 28, 2012 and accepted August 12, 2012.

Published online August 12, 2012
10.1021/nn301368z

In this review, the terms "nanopore" and "nanochannel" will be found since, at present, they are in common mutual use, so it is important to clarify first the differences between both structures. In terms of shape and dimensions, nanopore is defined as a pore having a diameter of 1−100 nm and being this diameter larger than its depth. When the pore depth is much larger than the diameter, the structure is generally called nanochannel. Therefore, nanochannels present a better selectivity on the transported molecules compared to the nanopores.[13]

Some recent reviews have described in detail the strategies for the integration of nanochannels, from ion channels to the fully synthetic nanochannels.[14−16] Insertion/integration of biological/natural ion channels into lipid bilayers, forming a biological ion channel, represents the pioneer strategy. The performance of this outstanding sensing system has even been improved by building solid-state/artificial nanochannels embedded in chemically and mechanically robust synthetic membranes, using various materials and technologies. These strategies will be discussed in detail in the following sections, giving a critical view of the main advantages and drawbacks of each one and focusing always on the objective to be used in biosensing applications.

VOCABULARY: Coulter counter - device used for counting and sizing particles suspended in electrolytes. Typically consists of one or more microchannels that separate two chambers containing electrolyte solutions. As fluid containing microparticles or cells is drawn through each microchannel, each particle causes a brief change to the electrical resistance of the liquid which is detected and related with the identity and concentration of the analyte; **α-hemolysin** - protein from the family of the hemolysines, exotoxins produced by bacteria that cause lysis of red blood cells *in vitro*. Its 3D structure usually consists of heptameric or octomeric pores, depending on the bacteria. This structure is extensively approached for the building of biological ion channels by the insertion of the α-hemolysin into artificial membranes, mainly lipid bilayers; **solid-state ion channels** - nanochannels used as an alternative to solve the problems of fragility of the biological ones, consisting of artificial nanochannels embedded in chemically and mechanically robust synthetic membrane; **stochastic sensing** - sensing method derived from the Coulter counter concept. It consists of the use of a single nanochannel-based platform, based on a synthetic or biological membrane as a resistive-pulse sensor for the detection of molecular and macromolecule analytes. It entails mounting the membrane containing the nanochannel between two electrolyte solutions, applying a transmembrane potential difference, and measuring the resulting ion current flowing through the electrolyte-filled nanochannel.

BIOLOGICAL ION CHANNELS

Nature structures have inspired laboratory research for many years. Bioinspired materials have attracted great interest because of their unique properties which have given rise to many applications.[17,18] For example, ion channels play important roles in living organisms, maintaining normal physiological conditions, responding directly to molecules or to some physical stimuli, and serving as "smart" gates to ensure selective ion transport. They also exhibit selective ion conduction and the ability to gate-open in response to an appropriate stimulus. Furthermore, in these natural ion channels, the ionic current flows through, and this current is altered when a molecule binds to a specific region of the channel.[19] All of these fundamentals are being approached for biosensing purposes, by using biological biomimetic nanochannels, simulating this natural behavior.[20,21]

Protein Channels. The protein ion channels used for the first time in real experimental approaches for sensing were the K^+-selective ion channel,[22] the channel formed by *Staphylococcus aureus* α-hemolysin,[23] and the channel formed by *Bacillus anthracis* protective antigen[24] (Figure 1B). Between them, the most widely used for biosensing is the α-hemolysin bacterial protein pore that consists of a structure formed by self-assembly of seven identical polypeptides from *Staphylococcus aureus*[25] (Figure 1C). The mushroom-shaped heptameric α-hemolysin pore consists of a 14-stranded transmembrane β-barrel (a large β-sheet that twists and coils to form a closed structure in which the first strand is hydrogen bonded to the last) and a bigger cap region which is positioned outside the membrane.[26] The external dimensions of the pore are 10 × 10 nm, and the inner diameter of the central channel varies between 2.9 nm at the cis entrance, 4.1 nm in the internal cavity, 1.3 nm at the inner constriction, and 2 nm at the trans entrance of the β-barrel (Figure 1C). The detection of analytes through nanochannel blockages against uchanging current levels is facilitated by the robust structure of the α-hemolysin protein, which results in a unitary conductance due to the lack of mobility.

Other examples of protein pores used for sensing are the porins such as the OmpG porin (a monomeric pore from the outer membrane of Gram-negative bacteria)[27] and the MspA pore from *Mycobacterium smegmatis*[28] or peptide antibiotics such as gramicidin and alamethicin.[29−31]

Insertion in Lipid Bilayers. The most often used biological nanochannel is the α-hemolysin protein channel. The typical sensor that resulted from this nanostructure consists of a single channel embedded within a lipid bilayer membrane. Traditionally, lipid bilayers are formed across 30−100 μm sized orifices in polysulfone, Delrin, Teflon, or other hydrophobic polymer-based membranes.[32] Then a single pore is inserted by

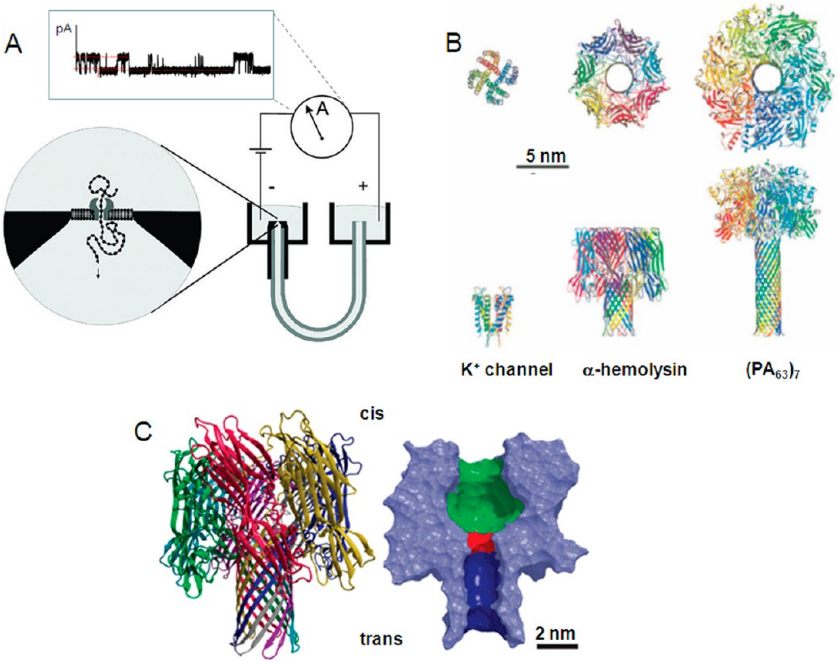

Figure 1. Biological ion channels. (A) Scheme of a nanochannel sensor based on the concept of the Coulter counter. Adapted with permission from ref 11. Copyright 2003 Oxford University Press. (B) Structure of the main protein ion channels applied in sensing. Adapted with permissiong from ref 21. Copyright 2008. (C) Detailed structure of the heptameric α-hemolysin channel. The cross-sectional view on the right displays the inner cavity (green), inner constriction (red), and β-barrel (blue). Adapted with permission from ref 25. Copyright 2009 RSC Publishing.

adding the protein solution to the chamber filled with the electrolyte.

In order to solve problems related to the lack of precise control of the channel insertion, alternatives consisting of the use of a hand-operated hydrogel probe which can be coated with a layer of proteins and mechanically engaged with the lipid bilayer have been more recently reported.[33,34] Furthermore, the stability of the bilayer has been improved by using soft or hard support structures. For example, supports made of soft hydrogels have been tested with photopolymerizable polymers,[35] poly(ethylene glycol),[36] and agarose gel.[37] Finally, the reduced diffusion and convection-based transport of analyte molecules through the support layer is also improved using solid supports, comprising the covalent linking of the bilayer to a support made of gold.[38,39] Solid support structures have also been implemented without chemical linkage, using porous alumina to stabilize pore-suspended lipid bilayers.[40] In order to obtain a tight interface between the membrane and alumina, a polymer cushion between the solid support and lipid bilayer was used.[41]

Biosensing Using Biological Ion Channels: Stochastic Sensing. *Sensing Principle.* A single nanochannel-based platform can be used as resistive-pulse sensor for the detection of molecular and macromolecule analytes. The resistive-pulse method, which when applied to such analytes is sometimes called stochastic sensing, entails mounting the membrane containing the nanochannel between two electrolyte solutions, applying a transmembrane potential difference, and measuring the resulting ion current flowing through the electrolyte-filled nanochannel. The structure and the physical processes affecting the ions' diffusion on biomimetic natural ion channels have been extensively studied in the past decade.[42−47]

In simplest terms, when the analyte enters and translocates the nanochannel, it transiently blocks the ion current, resulting in a downward current pulse. In fact, the transport of molecules across membranes is a key mechanism for many life processes. Molecules are usually very long (*i.e.*, DNA, RNA, proteins) in comparison to the diameter of the channels in the membranes which makes passage of their single unit difficult, provoking their translocation through the channels. Translocation is a complicated process whose dynamics are strongly affected by a variety of parameters such as the membrane thickness, membrane adsorption, electrochemical potential gradients, chemical potential gradients, and assisting molecular motors between others.

From the sensing point of view, the translocation of a molecule through a channel modifies the channel's electrical impedance, changing the ionic current which can be recorded and related to the molecule (analyte) and its concentration. Concretely, the mean duration and amplitude of the events are related to the identity of the analyte, while the frequency of occurrence of the events can be related to its concentration[48] (Figure 2A).

Detection of DNA, Proteins, and Other Analytes. The specificity of these natural protein pore-based sensors to a high variety of analytes can be achieved through

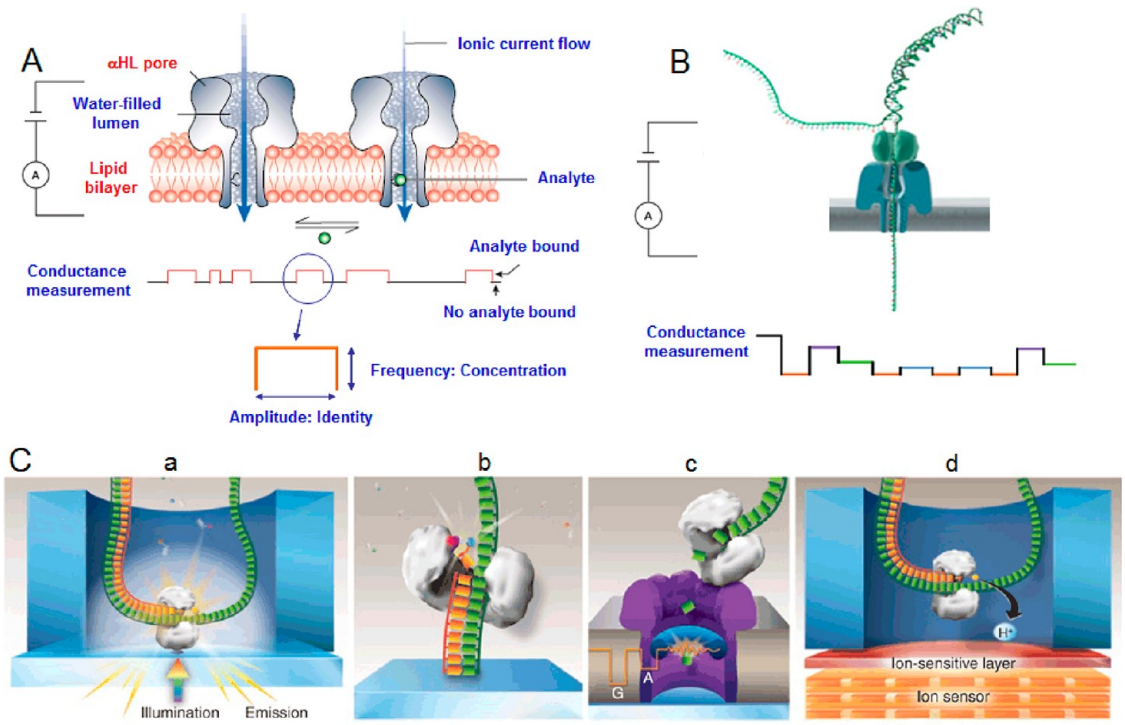

Figure 2. Stochastic sensing. (A) Schematic representation of the sensing using an engineered α-hemolysin protein nanochannel inserted in a lipid bilayer membrane. The different conductance between the two sides of the membrane in the absence (left) and presence (right) of an analyte in the sample allows its detection and quantification. Adapted with permission from ref 48. Copyright 2001 Nature Publishing Group. (B) α-Hemolysin pore as a potential tool for DNA sequencing. The DNA strand enters through the pore (above), and each of the four different bases of DNA could produce characteristic time series recordings (below). Adapted with permission from ref 21. Copyright 2008. (C) Third generation DNA sequencing systems developed by (a) Pacific Biosciences SMRT, using DNA polymerase and differentially labeled nucleotides, (b) Life Technologies Corp., using base fluorescent labeling technology, (c) Oxford Nanopore Technologies, using an exonuclease coupled to a modified α-hemolysin nanopore (purple, pictured in cross section) positioned within a lipid bilayer, (d) Ion Torrent sequencing platform, using an ion-sensitive layer and an ion sensor. Adapted with permission from ref 73. Copyright 2010 Nature Publishing Group.

the insertion of specific receptors using genetic engineering fabrication techniques. For example, metal ions can be detected after the insertion of histidines by amino acid replacement or substitution,[49] while single-stranded DNA and proteins can be detected after the immobilization of the corresponding bioreceptors on engineered nanochannels, including also genetically encoded sensor elements.[50]

The DNA hybridization event can be detected by covalently attaching inside the pore the oligonucleotide probe complementary to the target with interest to be detected. The DNA duplex formation produces a change in the ionic current which allows identification of the target ssDNA strand even at single-base resolution.[51,52] The resolution of the currents associated with individual nucleotides can be improved by immobilizing DNA strands inside the α-hemolysin pore through terminal hairpins or biotin−streptavidin complexes.[53,54]

In the DNA analysis field, efforts in the development of nanopore-based microRNA deserve to be highlighted. Outstanding is the work recently reported by Wang *et al.*,[55] where an α-hemolysin pore is used to selectively detect microRNAs at the single molecular level in plasma samples from lung cancer patients without the need to use labels or microRNA amplification. By using oligonucleotide probes, microRNA is captured in the pore generating a target-specific signature signal which allows one to quantify subpicomolar levels of cancer-associated microRNAs and distinguish single-nucleotide differences between microRNA family members.

Regarding the protein detection, one important problem found was related to the large protein length which inhibits their binding within the lumen of the α-hemolysin pore, so it was necessary to find a system able to detect binding events occurring outside of the pore. Several approaches have been reported that try to solve this, by using, for example, polymers bound within the pore but with a free ligand able to recognize proteins out of the pore. In this case, the protein recognition produces a decrease in the fluctuations of the polymer within the pore, registering a decrease in the current noise.[56] Other approaches used disaccharides attached close to the entrance of the pore, which are able to detect lectins by registering a decrease in the ionic current.[57] Other alternative strategies consisted of immobilizing inhibitor peptides

close to the entrance of the α-hemolysin pore, making the modified pore able to detect protein kinases through the blockage in the registered current.[50,58] Of special relevance is the approach very recently reported by Bayley and co-workers using aptamers as bioreceptors.[59] They first covalently attached to a single cysteine residue near a mouth of the pore, an oligonucleotide complementary to the aptamer through a disulfide bond. The aptamer was immobilized through the hybridization reaction, and then they observed that the presence of thrombin in the sample gave rise to the formation of a cation-stabilized quadruplex, which changed the ionic current through the pore, allowing detection of thrombin at nanomolar levels.

Furthermore, it must be highlighted that nanoscale channels have also been used, to a minor extent, as useful tools for single-molecule analysis of DNA or RNA processing enzymes[60,61] and to study peptides and unfolding of proteins.[62−64] Finally, noncovalent adapters can also be used to create binding sites for the detection of drugs and organic solvents.[65]

Potential Tool for DNA Sequencing. One of the more exciting perspectives in this field is the potential ability of the α-hemolysin nanopore for DNA sequencing. DNA single strands could be electrophoretically driven through the α-hemolysin pore[66] and pass in an elongated conformation generating a "fingerprint"-like blocking of the ionic current, which would be specific for each strand. The transit time and extent of the current could reveal information about the length of the nucleic acid and its base composition[21,67,68] (Figure 2B). On the other hand, the magnitude of the conductance changes could give additional details such as the presence of mismatches in DNA sequences. A key advantage of nanopore sequencing would be that it could detect nucleotides directly, without reagents or labeling, from a single molecule of single-stranded DNA, in contrast with the established techniques that require the use of fluorescent or luminescent labels, even also requiring the DNA amplification by the polymerase chain reaction. Furthermore, nanopore-based analysis is also potentially capable of sequencing much longer continuous strands of DNA than other techniques. This is of great importance for the analysis of long-range genomic complexity which is related to cancer and other diseases.

However, for the successful achievement of these purposes, a method of controlled translocation of the strand through the channel is needed together with a system that is able to solve the problems related to the fragility of the bilayer membrane that houses the nanochannel and the too short lifetime of these membranes (only a few hours before rupture).[69]

The membrane fragility problem has been very recently solved by approaches using hybrid biological/solid-state ion channels formed by a channel-forming protein set in synthetic material.[70] In this context, Oxford Nanopore Technologies has very recently presented a commercial system (GridION platform) which combines the α-hemolysin pore (inserted in synthetic materials) with the use of processive enzymes which ratchet DNA through the pore, showing that the method can be used to read lengths of many tens of kilobases. They have overcome also the problem derived from the fact that when a DNA polymer passes through a nanopore, a number of individual DNA bases occupy the aperture of the nanopore at any time. This company has engineered bespoke nanopores and data analysis algorithms to translate the characteristic electronic signals into DNA sequence data. The same company has also developed an alternative strategy based in the use of exonuclease enzymes which cleave individual DNA bases from a DNA strand.[71] Since the unmodified α-hemolysin channel is not able to differentiate DNA bases, they chemically modified the nanochannel by covalent attachment of cyclodextrin, which acts as a binding site for individual DNA bases and allows accurate measurement of their passage through the nanopore binding.

To improve the efficiency of these nanochannel sensors, Bayley and co-workers[72] have also recently reported the concept of a multibase recognition site in a single α-hemolysin nanopore, using two reading heads (R1 and R2) instead of only one. The current signal can consequently offer information about two positions in the sequence. It means that each base is read twice, first at R1 and second at R2, improving the overall quality of sequencing.

On the basis of all of these principles, third generation sequencing platforms have recently been commercialized by that and other companies, also taking advantage of labeling technologies[73] (Figure 2C).

Sensing with Arrays of Biological Ion Channels. A single nanochannel is an excellent system for studying transport properties of different ions or molecules since the behavior of a single channel can be observed directly, without having to average the effects of multiple channels. However, as a single nanochannel can probe only a single molecule at a time, strategies for manufacturing arrays of nanochannels able to detect different molecules and simultaneously monitor them are required. The difficulty here of simultaneous measurement of the ionic current in a high number of channels on the same membrane limits this kind of multianalyte detection. From the few examples of biological nanochannel arrays used for electrochemical biosensing, the work done by Osaki *et al.*[74] is outstanding, which is in fact also one of the few examples of application of the stochastic sensing principle to nanochannel arrays. They reported a microarray system that enables simultaneous monitoring of multiple ionic currents through transmembrane α-hemolysin nanopores arrayed at bilayer lipid membranes (Figure 3). The developed system is able to

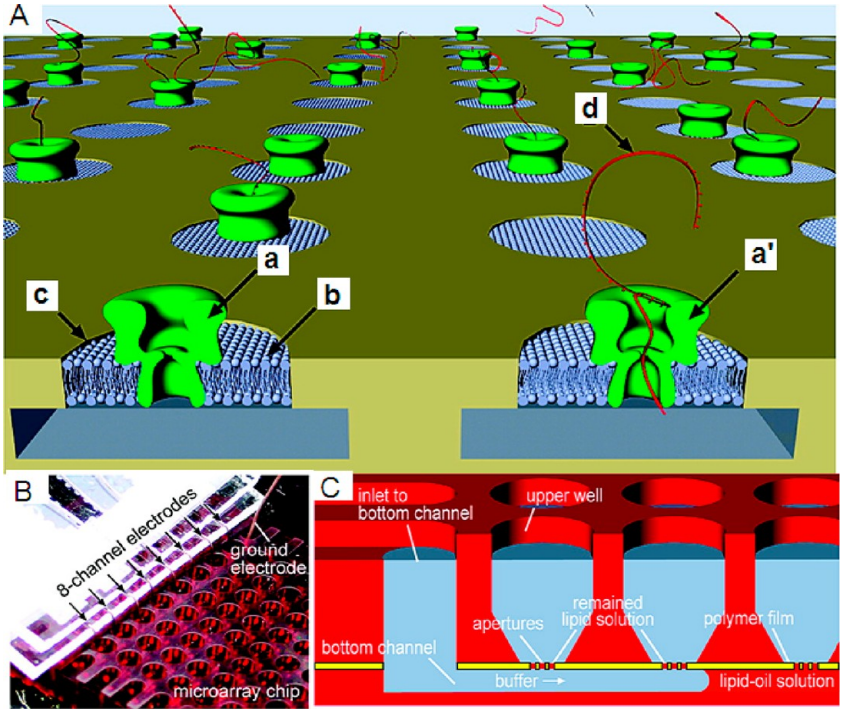

Figure 3. α-Hemolysin nanopore array. (A) Schematic diagram of the system that enables detection of multichannel signals from translocations of single molecules at the α-hemolysin nanochannels. Ionic current through a nanochannel is significantly reduced with the translocation of a single linear polymer such as ssDNA/RNA (a, α-hemolysin nanopore; a′, α-hemolysin nanopore blocked by a translocating molecule; b, bilayer lipid membrane; c, micrometer-sized aperture; d, analyte polymer). (B) Experimental setup of multichannel recording. (C) Cross-sectional image of the device. Adapted from ref 74. Copyright 2009 American Chemical Society.

detect translocation events of nucleic acid molecules, opening the way for further high-throughput applications. However, the difficulty of creating homogeneous arrays has limited their application for routine analysis.

As a conclusion of this first part of the review, it can be stated that, in spite of the advantages of the biological ion channels in terms of sensitivity, selectivity, and ability for the analysis of a variety of analytes, next generations of these sensing devices are likely to use nanochannels generated from synthetic materials, the so-called solid-state nanochannels, which are previewed to improve not only the cost but also the scale of analyses.

SOLID-STATE NANOCHANNELS

As stated before, the next generation of biosensing systems using nanochannels takes advantage of artificial nanochannels embedded in a chemically and mechanically robust synthetic membrane. Moreover, the length control that can be exerted on their fabrication allows one to improve parameters related to the signal detection and quantitative analyses by simply changing the length of the channel.[19,75] In addition, their size and shape can also be controlled in a precise way, that is, by metered penetration or ion track-etching technology, giving rise to conditions quite similar to the physiological ones. Furthermore, most of the developed methodologies for the generation of solid-state ion channels give rise to arrays of nanochannels (nanoporous membranes). This opens the way to novel large-scale real-world biosensing systems, different from those based in the concept of the Coulter counter, but with enormous potential not only due to electrochemical detection but also taking advantage of optical properties of such materials. In the following sections, the main methodologies for the preparation of both single/arrays of solid-state nanochannels for biosensing applications, their characterization methodologies, and both electrical and optical applications are detailed.

Preparation of Solid-State Nanochannels. The traditional basic methods for the preparation of porous materials consist of (i) aggregation of particles, (ii) subtraction of a component from a compact body, (iii) structural changes like crystallization, and (iv) inflation of a structure, for example, by swelling. There are also some special methods such as (i) compaction of powder, (ii) chemical reaction and precipitation, (iii) crystallization, and (iv) thermal treatment.

However, only a few of these basic methods were found to be useful for the fabrication of nanochannel-based sensors. The suitable materials are limited due to the requirements of stability, robustness, possibility of (bio)functionalization, and control of the pore size and distribution. In this context, the implementation of metal nanoporous polymer materials by electroless deposition made by Martin and co-workers,[76] followed

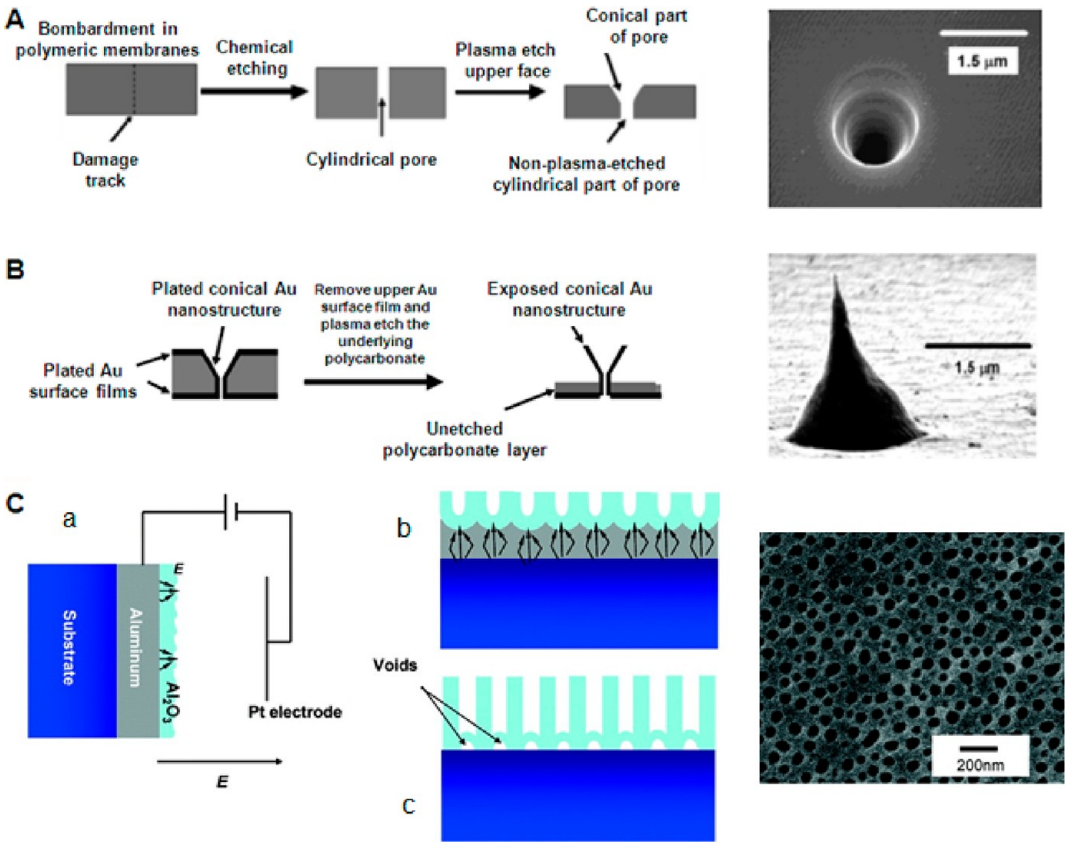

Figure 4. Preparation of solid-state nanochannels for sensing applications using the track-etch method (A,B) and metallic substrate anodization (C). (A) Scheme of a conical nanochannel generation and the corresponding SEM image. (B) Scheme of a gold conical nanochannel formation and the corresponding SEM image. Adapted from ref 91. Copyright 2004 American Chemical Society. (C) Left: Schematic of anodized aluminum oxide (AAO) template formation on ITO glass. Shown are (a) schematic of the setup system and (b) process of acidic dissolution of the native aluminum oxide as well as (c) the formed layer after the anodization process. Right: SEM image of the obtained pores. Adapted from ref 103. Copyright 2008 American Chemical Society.

recently by other groups using electron-beam evaporation[77] and ion sputtering,[78] opened the way to extensive research in this field, with the most successful strategies as follows: (i) track-etching on polymeric membranes; (ii) electron-beam lithography and ion beam sculpting: focused ion beam (FIB) and dual FIB/SEM systems; (iii) nanopore electrode fabrication from Pt wires; (iv) metallic substrate anodization; (v) micromolding and (vi) high ordered mesoporous thin films formation. The obtained nanochannels are often modified with other materials, particularly, their modification with graphene that takes advantage of the properties of this nanostructured material.[79,80]

Track-Etching on Polymeric Membranes. The pioneering method to produce both single/arrays of solid-state nanochannels was the track-etch method. The variations of this method and the use of membranes made of a variety of materials were recently summarized by Gyurcsány,[81] so we only highlight here the main aspects related to this method.

The pioneering works used as template material commercially available polycarbonate track-etch membranes of around 6 μm thickness. This method consists of bombarding the membrane with a collimated beam of high-energy nuclear fission fragments[82] or with ion beams from accelerators to create parallel damage tracks. The damage tracks are then etched into monodisperse pores by exposing the tracked film to a solution of aqueous base (Figure 4A, left). The diameter of the pore is determined by the etch time and the etch solution temperature, and the pore density is determined by the exposure time to the fission fragment beam. Membranes obtained with this method are nowadays commercially available, containing pores with diameters down to 10 nm and pore densities of approximately 6×10^8 pores cm^{-2}.

Multichannel nanopores for applications in biosensing can also be prepared in other materials such as anodized Al_2O_3 (AAO),[83−85] SiO_2/SiN,[86] and mesoporous silica MCM-41[87] as explained in following sections.

A great enhancement in the rate of transport through the membrane can be obtained using conical nanochannels[88] instead of cylindrical ones. These conical shapes are obtained doing an asymmetric etching that places only one side of the membrane in contact with the etchant (Figure 4A, right). The geometry and

size of the cones have been controlled following different strategies such as the addition of additives[89] or the application of hydrostatic pressure.[90] These conical nanochannels can be filled with, for example, gold in order to obtain gold nanoelectrodes with radii down to 2 nm[91] (Figure 4B).

However, these track-etch membranes do not offer pore sizes in the range of 10−100 nm, where the most interesting nanomaterial properties are exhibited. Moreover, these templates do not offer much control over the morphology of the nanostructures synthesized in them; the pores are randomly distributed and are rather toothpick shaped with correspondingly difficult control and understanding of the nanomaterial properties synthesized in them. In addition to the above disadvantages, these materials are expensive to produce and attempts to rectify the morphological disadvantages have only led to increased production costs.

The physicochemical modification of the inner surface of track-etched polymer nanochannels is of key importance for further biosensing applications. Modification with metals such as Au and Pt (by electroless deposition, ion sputtering, and electron-beam evaporation) or polymers (by initiated chemical vapor deposition and plasma) as well as the final introduction of biomolecules such DNA and antibodies has been extensively reported. These modifications after symmetric/asymmetric design for the shape of nanochannels have been very recently summarized and described in detail by Jiang's group[92] and so will not be considered in this review.

Electron-Beam Lithography and Ion-Beam Sculpting: Focused Ion Beam (FIB) and Dual FIB/SEM Systems. Another approach with a high degree of pore-size control consists of the electron-beam lithographic generation of the pores on Si membranes,[93] taking advantage of a high-energy electron beam provided by commercial TEM/SEM devices. In spite of the advantages of this technique in terms of the high resolution achieved, it has the limitations of slow serial process and a small area that can be patterned.

An important step here in single solid-state nanochannel fabrication was made with the development of the ion-beam sculpting method which bridges nanochannel sensing and well-established materials and procedures used in microelectronics.[94] Nanochannels generated using the focused ion-beam (FIB) milling can be tailored down to less than 5 nm in diameter.[95] A variety of noble gas ions and ion-beam fluxes (He, Ne, Ar, Kr, and Xe) have been used to drastically change some of the potentially relevant parameters of the process.[96]

The actual FIB machines are increasingly equipped with an electron beam (the so-called dual-beam or cross-beam machines) that allows the electron beam to be used also for imaging, like in conventional SEMs.[97,98] A mini-RF-driven plasma source can be used to generate a focused ion beam with various ion species. A two-lens electron column can be used for SEM imaging, and finally, an axis manipulator system can be used for sample positioning. This kind of integrated FIB/SEM dual-beam system not only helps to improve the accuracy and reproducibility when performing ion-beam sculpting but also enables one to perform cross sectioning, imaging, and analysis with the same tool. The main advantage of this approach is the ability to produce a wide variety of ion species tailored to the application. In this context, the implementation of a helium ion microscope (HeIM) as a potential technique for precise nanopatterning is one of the latest innovations in this area,[99] related to its ability to mill and sputter soft materials, in particular, low atomic number materials with extremely low rates with an extremely small probe size on the order of 0.5 nm.

Although the prospects are promising, the high cost and times of production of these techniques minimize their extensive use for nanochannel fabrication and further biosensing purposes.

Nanopore Electrode Fabrication from Pt Wires. In contrast with the single solid-state nanochannels fabricated in a free-standing form, the nanopore electrodes fabricated from Pt wires have only one end of the nanopore opened to the solution, whereas the other end is backed by the electrode material. Such nanopore electrodes are fabricated by sealing an electrochemically etched Pt wire into a glass capillary, with the glass polished and finally the generated Pt disk (diameter of around 15−100 nm) electrochemically etched back.[100]

The advantages of this design include the simplicity and reproducibility of fabrication, a built-in signal transduction element (the Pt electrode) for monitoring molecular transport through the pore, and the portability and mechanical robustness of the solid electrode.

Metallic Substrate Anodization. Another very interesting fabrication technique consists of the nanochannel array generation on metallic substrates, with the most representative one being the generation of such nanochannels on aluminum. A typical fabrication process[101] consists of the anodization of aluminum of high purity in an acidic solution applying a constant high voltage. Under these conditions, aluminum oxide is generated, containing many surface irregularities (defects) where the electric field concentrates. This localized electric field enhances acidic dissolution of the oxide at the bottom of the pores while leaving the pore walls intact, resulting in the nanochannels' formation. The barrier layer produced at the bottom of the pore channels is subsequently removed by immersion in dilute acid during which the pores are also enlarged. The anodization under optimized conditions gives rise to the production of porous alumina with a highly ordered cell configuration. Moreover, a two-step anodization process for fabricating self-ordered porous alumina templates was pioneered by Masuda's group.[102]

These alumina (Al_2O_3) membranes with a variety of pore sizes are nowadays commercially available, and their advantageous properties have made possible their extensive use for biosensing applications, as will be detailed in the *applications* section.

An exciting alternative of special interest also for later biosensing applications consists of the generation of Al_2O_3 nanochannels directly on the surface of an electrotransducer surface, which has been recently reported by Foong *et al.*,[103] after depositing an aluminum layer by chemical vapor deposition (Figure 4C). However, the use of this kind of high vacuum techniques is expensive and time-consuming. An alternative that overcomes these drawbacks consists of *in situ* electrodeposition of the aluminum on the surface of an electrotransducer. Unfortunately, the electrodeposition of aluminum from metal aqueous solution is not possible, due to the hydrogen discharge produced at the high negative potentials needed (below −1.67 V *vs* NHE). In order to solve this problem, ionic liquids, a new class of compounds characterized by high conductivity, low vapor pressures, and wide electrochemical windows, were found to be ideal media for the electroreduction of highly positive metals which cannot be electrodeposited from aqueous media. In this way, 1-butyl-3-methylimidazolium heptachloroaluminate[104] and 1-ethyl-3-methylimidazolim chloride[105] were used as the source of aluminum for its electrodeposition on carbon steel and further generation of nanochannels by anodization. However, in spite of the above-mentioned advantages, it deserves to be pointed out that the aluminum electrodeposition from ionic liquids requires a dry atmosphere to avoid the presence of H_2O in the liquid, as this would be a handicap for routine fabrication.

Finally, another example of metal substrate anodization that deserves to be mentioned consists of the preparation of an alloy of nickel, electrolytic aluminum, and rhenium pellets, melting under an inert atmosphere and drop-casting into a cylindrical copper mold.[106] Then, the production of nanochannel arrays is performed by electrochemical anodization/dissolution of the rhenium fibers, obtaining the pores. Furthermore, metals such as gold can be deposited inside them to give a nanoelectrode array that might prove to be useful in electrochemical sensors.

Micromolding Techniques. Micromolding from PDMS. Artificial nanochannel arrays for molecular sensing can also be fabricated with great ease and control using micromolding techniques. Well-established lithographic techniques are used to create a negative master of the pore and reservoirs, which is subsequently cast into a poly(dimethylsiloxane) (PDMS) slab, as done by Saleh *et al.*[107] They created the negative of the pore on silicon substrates by patterning a 200 nm sized (wide and thick) polystyrene line using electron-beam lithography and then used photolithography to pattern a photoresist (SU-8) on the substrate to form the negatives of the reservoirs. The outstanding durability of both polystyrene and SU-8 after the cross-linking allows the reuse of the masters indefinitely.

Micromolding from Block Copolymers. An improvement of the previous approach consists of the fabrication of well-defined nanostructures for nanopatterning using self-assembly of block copolymers (BCPs), which is of great interest due to the flexibility, simplicity, and low-cost of the process together with the possibility of tuning the dimensions and chemical properties. Many potential applications of BCP thin films to different nanotechnologies, such as the BCP lithography,[108] nanoparticle template,[109] nanoarrays,[110] and nanoporous thin films,[111] have been developed. Poly(methylmethacrylate) (PMMA) homopolymers[112] and polystyrene-*b*-polydimethylsiloxane (PS-PDMS) block copolymers have recently been used for the formation of well-oriented cylinders with perpendicular morphology.[113]

As it has been mentioned, these emerging materials have enormous potential but the easy formation of cracks and film delamination must be taken into account, problems that must be solved for the massive implementation of this fabrication method.

Soft Lithographic Molding: Nanoimprint Lithography. The recent advances and improvements in the soft lithographic molding in terms of both the absolute sizes and aspect ratios of molded features that it can generate have made this technique an interesting alternative for the production of nanochannel arrays. On the basis of these fundamentals, Aizenberg and co-workers have demonstrated that replica molding can be used to transfer an array of high-aspect-ratio nanoposts from silicon to epoxy, through a PDMS intermediate[114] and also that, in combination with nanoskiving, these high-aspect-ratio structures provide a basis for the fabrication of arrays of significantly smaller and more complex structures, and in greater numbers of replicas.[115] The initial drawback of the cost of defining a master with nanostructures for soft lithography is offset by the ease and low cost of producing, for example, PDMS replicas for further experiments to fabricate nanostructures, which has allowed the implementation of the nanoimprint lithography[116−118] as a robust technique for nanochannel generation. Of special interest is the nanotransfer print concept very recently reported by Rogers and co-workers.[119] It consists of the use of stamps prepared on silicon wafers anisotropically etched through polymeric masks, defined by soft nanoimprint lithography, and final nanotransfer printing onto PDMS target substrates. In this way, they obtain 3D nanochannels on flexible substrates in a simple way and with mass production possibilities (Figure 5A).

However, in spite of the promising perspectives, other limitations have to be considered such as the softness of the PDMS that can cause distortions in

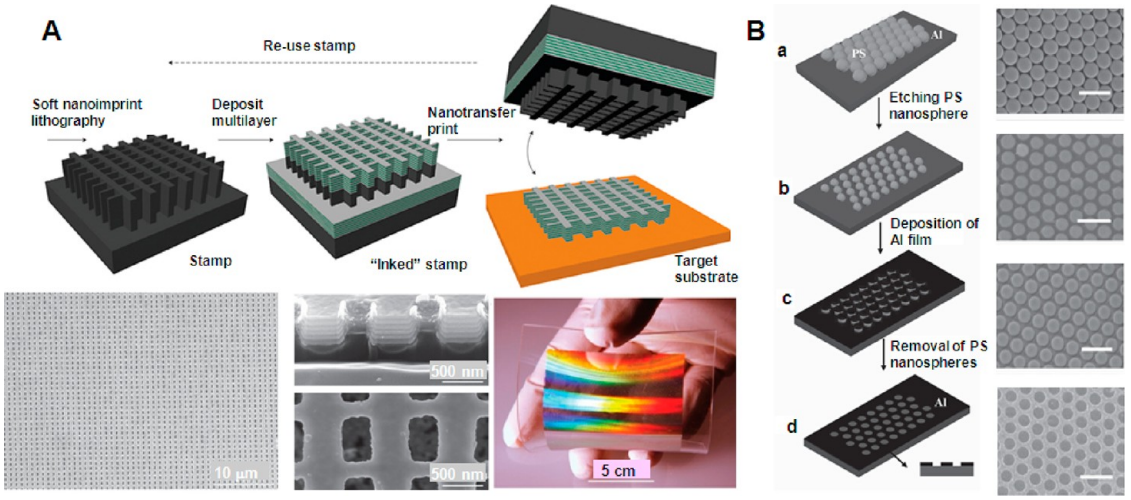

Figure 5. Fabrication of nanoporous films using block copolymers and nanosphere lithography. (A) Schematics for the formation of well-oriented cylinders with perpendicular morphology for PS-PDMS thin films and the corresponding FE-SEM image. Adapted with permission from ref 119. Copyright 2011 Nature Publishing Group. (B) Schematic diagrams and corresponding SEM images of the nanochannel formation by nanosphere lithography on aluminum substrates: (a) surface modification of an aluminum substrate with a close-packed polystyrene sphere monolayer; (b) loose-packed polystyrene sphere monolayer *via* the treatment of the O_2 reactive ion etching to increase the distance between each other; (c) loose-packed polystyrene sphere monolayer with a layer of aluminum through vacuum evaporation deposition method; (d) prepatterned aluminum substrate with a hexagonal nanoindentation array after polystyrene spheres are removed by ultrasonic treatment. The scale bars are 1 μm. Adapted with permission from ref 124. Copyright 2012 Wiley.

printed or molded structures and its instability in many organic solvents or at high temperatures.

Highly Ordered Mesoporous Thin Film Formation. The use of highly ordered mesoporous and macroporous thin films coating solid electrode surfaces has a great potential application in electrochemical analysis.[120] Strategies such as the use of self-assembled nanoparticle templates,[121] self-assembled surfactant templates,[122] and hard templating/nanocasting approaches[123] have been followed in the past years in order to get ordered nanochannel array films on electrodes.

Nanoparticle Assembling. The first strategy consists of assembling nanoparticles in a well-controlled way. The simplest approach is based on a simple evaporation of a thin film of nanoparticle suspension on the horizontal electrode surface under well-controlled conditions of temperature and humidity, obtaining locally well-organized structures. This method is therefore suitable for modifying electrodes with a small geometric surface area, as is the case for ultramicroelectrodes, but for electrodes with a surface area larger than square millimeters, vertical deposition is more suitable, allowing much better control of defect density. A very interesting variation of this technique consists of the so-called nanosphere lithography (NSL). Work very recently reported by Wang *et al.*[124] is of special interest; it consisted of the formation of a highly ordered and hierarchically structured anodic aluminum oxide template by first prepatterning an aluminum substrate surface with a nanoindentation array *via* polystyrene nanosphere lithography and finally performing an anodization treatment (Figure 5B).

Furthermore, the interstitial space between the beads can be filled with conducting material such as metals,[125] carbon,[126] and polymers[127] using electrodeposition and electropolymerization. The subsequent removal of the template results in the final porous structure, which is a perfect negative copy of the template.

The great advantages of this method in terms of simplicity, low cost, and versatility are minimized due to the formation of intrinsic defects observed at large scale that induce irreproducibility in further sensing applications.

Surfactant Template Assembling and Hard Templating/Nanocasting Approaches. Highly ordered mesoporous metallic films can be generated by electrodeposition utilizing lyotropic liquid-crystalline phases of nonionic surfactants (*i.e.*, polyethylene oxides) as a direct physical cast to template the mesostructure.[128] Furthermore, ordered mesoporous carbons with various pore structures can also be produced by a nanocasting process using mesostructured silica samples with a specific pore topology as secondary templates,[129] which involves the infiltration of a carbon precursor into the pores followed by transformation into a rigid carbon structure by pyrolysis and the removal of the silica template to obtain the mesoporous carbon replica.

Other interesting materials used for such application are porous silica (PSi), photonic architectures such as single- and double-layered Fabry-Pérot films,[130] and more complex multilayer Bragg mirrors,[131] rugate filters,[132] and microcavities.[133]

These approaches take advantage of the diverse structure and dimension of the template materials and the possibility to design the chemical composition and structure. However, there still remain challenges in

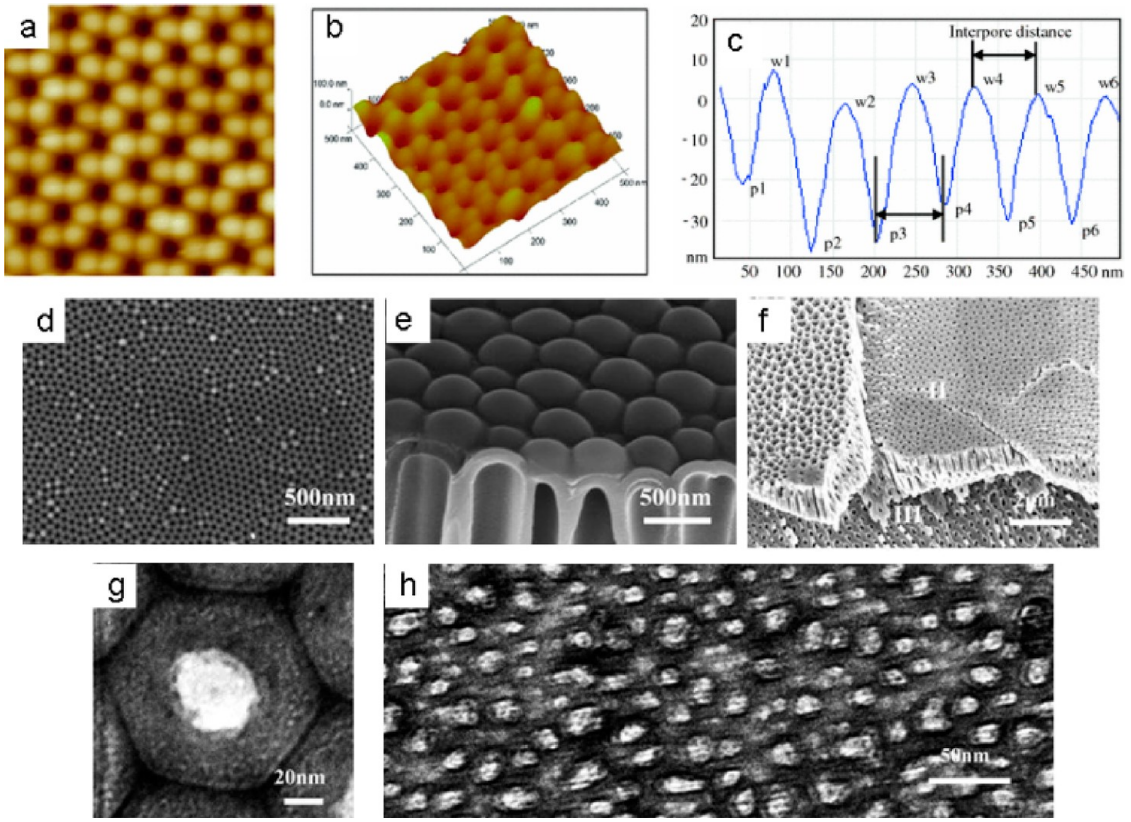

Figure 6. Characterization of porous anodic alumina using imaging techniques. (a) AFM image, (b) AFM three-dimensional structure, and (c) line profile analysis. (d) FESEM top view, (e) FESEM cross-sectional view, and (f) FESEM image of scratched membranes showing three different regions. (g) TEM of a single hexagonal cell and (h) top view of a membrane containing nanopores with diameters of 15 nm. Adapted with permission from ref 139. Copyright 2010 Springer.

their use arising from some inherent disadvantages related to the costly precursors needed and the required conditions of high temperature and inert environmental, which also increase the operational costs and the time of the process, limiting the mass production.

Characterization of Solid-State Nanochannels. The main methods used for the characterization of nanochannels, always from the perspective of the later biosensing application, will be described in this section. Although most of the methods are described here for the characterization of solid-state nanochannels, almost all of them are also valid for the study of biological ion channels.

Imaging Characterization. The thickness of the membrane and the pore size and shape (also their density and distribution in the case of nanochannel arrays) are crucial parameters that need to be accurately controlled in order to ensure a good and reproducible performance of the derived sensing systems. Imaging techniques, such as atomic force microscopy (AFM), transmission electron microscopy (TEM), and field emission scanning electron microscopy (FESEM), give an estimation of all of these parameters in a rapid and easy way. AFM[134] can only be used to observe the membrane surface but has the advantage of no requirements on the conductivity of samples and its high resolution below the nanometer level. FESEM[135,136] is widely used to observe the surface and cross sections and measure the thickness of different samples but requires good electrical conductivity, a problem that can be solved by sputtering conductive layers. Finally, TEM[137,138] can be used to observe cross sections and morphology and also to characterize composition and crystalline structures. These techniques, mainly SEM, are routinely used for a preliminary characterization of nanochannels, with remarkable and thorough characterization studies of typical porous anodic alumina membranes recently reported by Zhu *et al.*[139] using AFM, TEM, and FESEM, obtaining useful information about different channel generation strategies (Figure 6).

The main advantages of the nanochannel analysis by AFM compared with the one performed using electron microscopy techniques are related to the ability of providing a higher resolution, 3D surface profile and the non-necessity of neither special treatments (such as carbon/metal coatings) that could damage the membranes nor expensive vacuum environment. However, the AFM analysis has the well-known limitations related to the single scan image size (maximum scanning area of about 150 $\times$ 150 μm in one pass), low scanning speed, and the possibility of obtaining image artifacts induced by unsuitable tips between others.

Electrochemical Characterization. It is known that the conductance of the pores depends on membrane voltage, and this kind of dependence is related to the radius of the pore. More in detail, the nanopore current depends on the shape of the pore,[140] the pH of the solution,[141] the distribution of surface charges,[142] and the chemical composition of the ions.[143]

The dependence of the nanopore biosensor conductance signal on its shape is a very important factor to be taken into account. The 3D shape of a nanopore allows for modeling its conductance on a wide range of ionic strengths. Furthermore, recent studies[144] have demonstrated that the dependence of the nanopore conductance on ionic strength can be used to obtain precise information about the nanopore shape, avoiding the use of time-consuming imaging analysis, a reliable methodology to monitor and evaluate changes in the nanopore shape during electrical measurements.

From the biosensing point of view, the analyte diffusion through the nanochannels and the effect of the charges of both analytes and channels on this diffusion are fundamental parameters that have been studied through electrochemical measurements of resistance, conductance, voltammetry, or zeta-potential. As the Coulter counter concept is the basis of the sensing using single nanochannels, the characterization of such a device (in the micrometric scale) is a good starting point to understand the behavior of the nanometric devices.[145]

The electromechanical coupling due to the electrical charge separations at interfaces is of great importance in microfluidics, as this kind of coupling exploited, for example, the electro-osmotic reactant delivery in the total microanalysis systems.[146] Some of these macroscopic characteristics are still valid when changing from micro- to nanofluidics due the fact that the system dimensions are much larger than the molecular scale. The remarkable new phenomena expected to be found in the nanoscale are the formation of polarization due to mechano- and electrochemical couplings as well as the appearance of surface conductivity due to electrostatically adsorbed counterions. Those phenomena must be carefully considered while studying the transport properties of fine porous membranes. In such membranes, the analyte transference between channels is electrically implemented so that electro-osmosis is of great importance. In this context, the so-called zeta-potential, which controls the electromechanical coupling, is of crucial importance. In porous media, the zeta-potentials are obtained through the measurements of streaming potential,[147] but these measurements by themselves do not give a direct estimation of the zeta-potential, due to the interference exerted by electric layers overlapping. Due to that, electric conductivity has been extensively used as a parameter to control the etching process,[148] and in combination with streaming potential measurements, they also have been applied for the extraction of detailed information about the

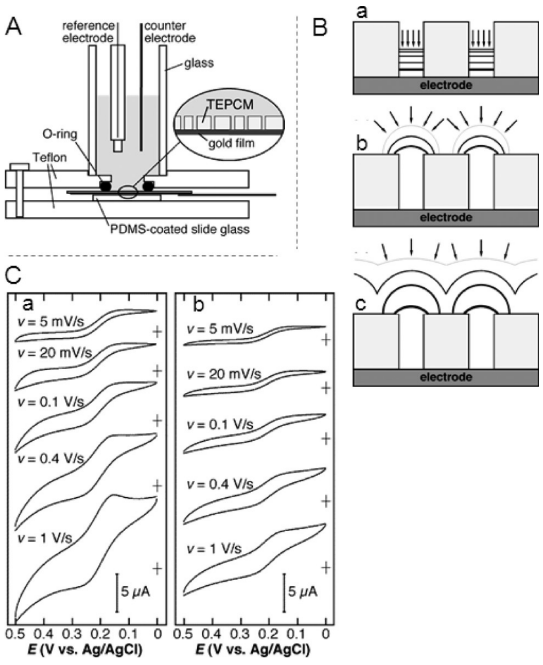

Figure 7. Nanochannel characterization using cyclic voltammetry. (A) Scheme of the electrochemical cell setup for track-etched polycarbonate membrane on a gold film electrode. (B) Scheme of the diffusional flux of molecules to the electrode at (a) fast, (b) low, and (c) very low scan rates. (C) Cyclic voltammograms obtained in 1.0 mM $K_3Fe(CN)_6$/0.1 M KNO_3 at five different scan rates (a) and the same for blocked nanochannels (b). Adapted from ref 153. Copyright 2006 American Chemical Society.

electrochemical properties of nanoporous membranes,[149] finding that the limiting current densities for a nanofluidic system are 2 orders of magnitude lower than the normal values found in microfluidic ones with electro-osmotic fluid delivery, an important handicap that must be taken into account in the application of such nanofluidic elements in microsystems.

The presence of charges in both analytes and nanochannel walls is a crucial parameter that affects the nanochannel-based sensing systems. The formation of the charges at a nanochannel inner wall is due to dissociation of surface groups or the adsorption of charged molecules from the solution.[150] The relative ratio between wall surface/channel bulk volume increases when the channel width decreases, giving rise to some adsorption effects. Consequently, the molecular and ionic species present in nanochannels suffer stronger interactions with the inner walls. The electric double layers formed at the inner walls can fill substantial parts of the nanochannels, which strongly affects the transport of molecules, the fluid flow, and the electric current.[151] In this context, reported conductance models in nanochannels with charged walls[152] demonstrate that relatively small concentration of wall charges dramatically reduces the self-energy transport barrier. These phenomena must be carefully considered by further applications of nanoporous materials in biosensing.

Simple voltammetric measurements can also be performed for the characterization of nanoporous materials. For example, cylindrical nanochannels, with a diameter of 50 nm, fabricated from track-etched polycarbonate membranes on gold films were characterized by Ito *et al.*[153] using cyclic voltammetry (CV) (Figure 7). The CV measurements showed the transition from linear to radial diffusion modes of redox-active species with decreasing scan rate. The resulting change in maximum faradaic current, which is the peak current in a peak-shaped CV and the plateau current in a sigmoidal CV, provides a simple means for calculating the pore length and effective pore density. Furthermore, nanopore electrodes fabricated from Pt wires were also voltammetrically characterized by White's group,[154] who performed computer simulations and detailed the steady-state response of the nanopore electrode.

Finally, the coupling of both electrochemical and optical measurements recently reported by Perry et al.[155] deserves to be highlighted, where they monitored also the ion transport nanofluidic funnels by measuring the fluorescence of fluorescein molecule flowing through the channels, opening the way to dual measurements of interest for many applications.

Nuclear Magnetic Resonance and X-ray Diffraction Characterizations. Nuclear magnetic resonance (NMR) spectroscopic techniques have been used to investigate the structure and adsorption properties of porous metal−organic materials.[156,157] These techniques can give useful information about the shape and size of the cavities in nanoporous materials.[158] For example, NMR spectroscopy is one of the most powerful techniques used for the characterization of the porous structure and the sorption mechanism in sorbents such as zeolites, organic host, and silica-based mesoporous materials.[159,160] In particular, multinuclear, two-dimensional (2D) solid-state nuclear magnetic resonance spectroscopy, which is sensitive to interatomic distances and dynamics, allows characterization of molecular structures.[161]

Furthermore, the spectroscopy of spin-active gases diffused to the nanochannels can also give useful information about the shape and size of the nanochannels. For example, xenon NMR spectroscopy has been used for the characterization of nanoporous materials.[162] By continuous flow technique, Xe can be continuously delivered to the sample, allowing the recording of 2D exchange spectra and collection of information on the accessibility of the nanochannels.

It can be stated that NMR techniques can be used in a complementary way to obtain a complete map of the analyzed material. In this context, Comotti *et al.*[163] reported the combination of multinuclear solid-state ^{129}Xe NMR, together with synchrotron X-ray diffraction and adsorption, to investigate the structural relationship and adsorption properties of an Al^{3+} microporous coordination polymer with straight 1D channels. Two-dimensional solid-state NMR spectroscopy, including $^{1}H-^{13}C$, also revealed the arrangement of the framework (Figure 8A). However, in spite of the above-mentioned advantages, NMR techniques are not extensively used for nanochannel characterizations, due to their limitations related to the expensive and time-consuming analysis that includes the relatively long period of times necessary for the interpretation of the spectra.

Grazing-incidence X-ray diffraction[164] is also a powerful technique used for the characterization of nanoporous materials. This technique uses small incident angles for the incoming X-ray so that diffraction can be made surface sensitive. It is used to study surfaces and layers because wave penetration is limited in the order of nanometers. This is the case in the work reported by Malachias *et al.*,[165] where X-ray grazing-incidence diffraction was used to confirm the crystalline quality of nanochannel networks fabricated by etching techniques (Figure 8B). However, the use of this powerful technique is limited to only materials with low stress gradient, due to the variability of the penetration depth which depends on the incident angle.

Other Characterizations. In addition to those detailed above, several other techniques, such as ellipsometric porosimetry[166] and X-ray porosimetry,[167] have been established over the past decade as capable metrologies to characterize pores in submicrometer thin films. These techniques are based on a variety of physics interactions between the probe and the pores. Both porosimetry techniques give useful information about the pore metrics in determined materials, but none of them is totally comprehensive for a full characterization of the pores. In this context, depth-profiled positronium annihilation lifetime spectroscopy (PALS) emerged as a unique porosimetry technique with broad applicability in the characterization of nanoporous materials.[168,169] PALS employs positrons, the antiparticle of electrons, to probe the pore structure of materials. Depth profiling with PALS has been proposed as an alternative methodology to study depth-dependent changes in porous structures without damaging the sample by injecting the positrons, for example, into porous films as reported by Peng *et al.*[170] However, this technique strongly depends on model assumption and is not accurate for pore size of less than 10 nm.

Finally, another technique used to a much lower extent but that deserves to be highlighted is the scanning ion conductance microscopy (SICM). This technique can be used to interrogate ion currents emanating from nanometer-scale pores of a polymer membrane as recently reported by Chen *et al.*[171] They measure the transport activity of individual pores by evaluating ion current images and simultaneously record the corresponding topographic images,

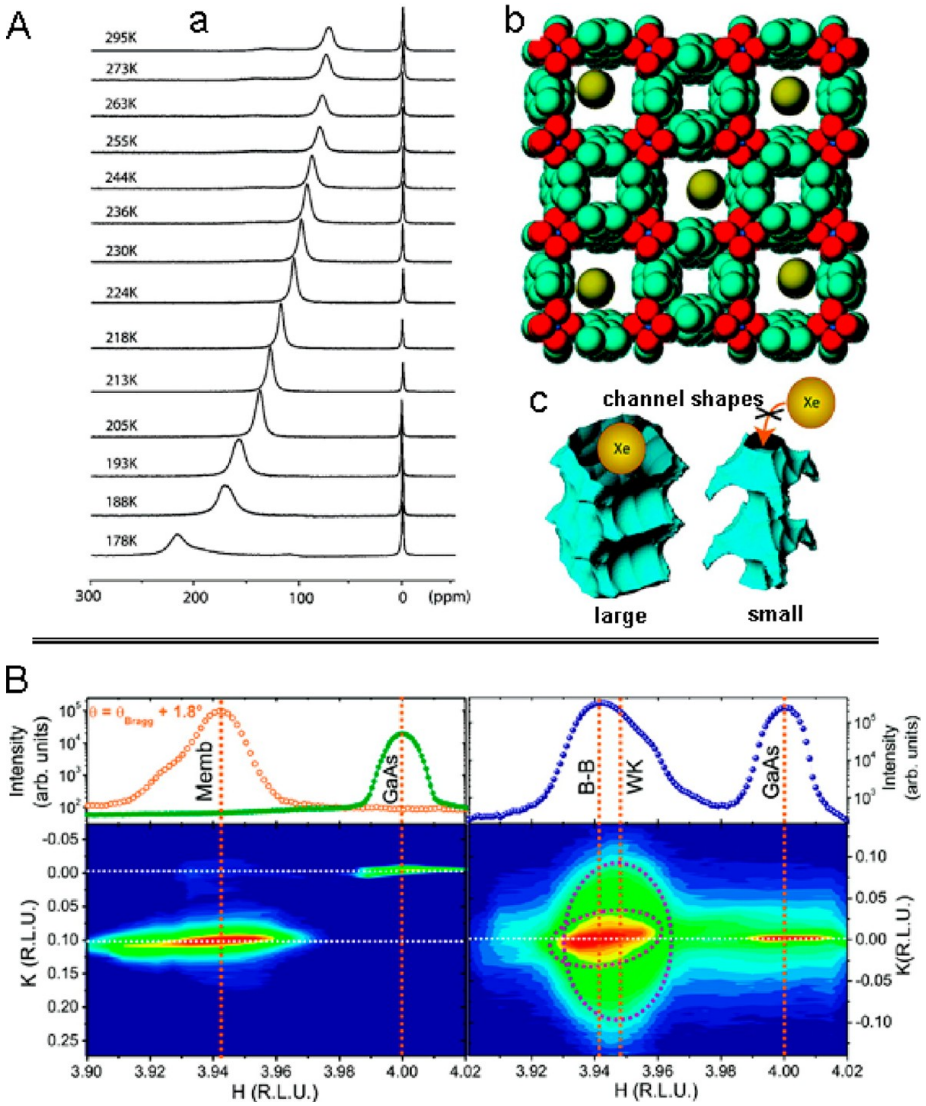

Figure 8. Nanochannel characterization using NMR and X-ray diffraction. (A) Continuous flow ^{129}Xe NMR spectra of a porous Al-based coordination polymer at variable temperatures (a); crystal structure of the same polymer, viewed along the channel axis (b); xenon atoms can diffuse in the large channels but cannot enter in the small channels (c). Colors are as follows: carbon, light blue; oxygen, red; aluminum, blue; xenon, yellow. Adapted from ref 163. Copyright 2008 American Chemical Society. (B) X-ray diffraction measurements of free-standing 20 nm thick $In_{0.2}Ga_{0.8}As$ nanomembrane. Adapted from ref 165. Copyright 2008 American Chemical Society.

concluding that nanoscale transport properties can be accurately measured with SICM.

Integration into Lab-on-a-Chip Platforms. Microfluidics and lab-on-a-chip systems have undergone enormous development during the past decade. The combination of such systems with nanochannels and other nanostructured platforms has opened the way to very promising integrated sensing devices.[172,173]

The most common fabrication method for such devices involves the use of sacrificial layers to prepare the nanochannels directly on the chip.[174] Using this strategy, even vertical arrays of nanochannels have been reported.[175] Another suitable method takes advantage of elastomeric substrates, where the master is obtained by introducing controllable cracks in an elastomer.[176] This method can be greatly simplified doing an injection molding of thermoplastic polymers, giving rise to well-defined nanofluidic systems in a single processing step.[177]

The conditions, however, have to be carefully optimized to obtain closed channels, as one of the major problems here is ceiling collapse, which blocks the nanochannels even during fabrication. There are only a few examples of nanochannels on glass chips, due to the fact that the etching of glass is mostly isotropic, as a result of which it is difficult to control the lateral dimensions of the channel in the nanometer range. In spite of these problems, the progress in this field has been far beyond the original micro total analytical systems because microfluidic devices are being used not only as analytical systems but also as platforms for bioreactions. However, the microfluidics research field

is still facing many challenges that prevent analytical application, such as the improvement of both selectivity and sensitivity parameters.

Electrical-Based Biosensing Applications. Although the most reported way to approach nanochannels for biosensing with final electrochemical detection consists of the application of the above explained Coulter counter principle using single nanochannels, some recent works have also focused on the use of nanochannel arrays, following in this case different sensing strategies, mostly based on the modification of conventional electrotransducer surfaces and measuring the changes in the electrochemical response of an electroactive species in solution. In all cases, these sensing methodologies take advantage of the inherent properties of the electrical techniques, such as the short time and costs of analysis and the easy to use modes between others. Some typical electrical-based applications related to the use of single nanochannels and the array-like ones are discussed in the following sections.

Use of Solid-State Single Nanochannels. A single nanochannel-based platform, based on a synthetic or biological membrane, can be used as resistive-pulse sensor for the detection of molecular and macromolecule analytes. The resistive-pulse method, which when applied to such analytes is sometimes called stochastic sensing, entails mounting the membrane containing the nanochannel between two electrolyte solutions, applying a transmembrane potential difference, and measuring the resulting ion current flowing through the electrolyte-filled nanochannel. In simplest terms, when the analyte enters and translocates the nanochannel, it transiently blocks the ion current, resulting in a downward current pulse (as detailed in previous sections). The current-pulse frequency is proportional to the concentration of the analyte, and the identity of the analyte is encoded in the current-pulse signature, as defined by the average magnitude and duration of the current pulses.

The structure and the physical processes affecting the ions' diffusion on biomimetic natural ion channels have been extensively studied in the past decade.[47,178−182]

Solid-State Single Nanochannel Functionalization. The functionalization of solid-state single nanochannels for further applications in most of the biosensing formats is a crucial step which is under extensive research. The biosensing capabilities of the nanochannels obviously depend on the surface characteristics of their inner walls to achieve the desired functionality of the biomimetic system. In addition to the classical functionalization methods, it deserves to be highlighted the novel approach recently reported by Ali *et al.*[183] to incorporate biosensing elements into polymer nanochannels by using electrostatic self-assembly. They used bifunctional macromolecular ligands to electrostatically assemble biorecongnition sites into the walls of single conical nanochannels generated in poly(ethylene terephthalate) (PET) membranes, which then were used as recognition elements for biosensing, opening the way to improved systems based on polymeric membranes. The recent approach reported by Jiang's group,[184] based on the modification of a solid-state single nanochannel with β-cyclodextrin for the enantioselective recognition of histidine enantiomers through monitoring of ionic current signatures, is also remarkable.

DNA Analysis. Cylindrical-shaped solid-state single nanopores generated in silicon nitride/oxide membranes by electron-beam lithography/ion-beam sculpting have been used to resolve sequences of individual DNA molecules linked to a degree of partial pore blockage by the DNA[185−189] measuring changes in conductance during DNA translocation. Al_2O_3 substrates with pores generated by electron-beam lithography[190] or ion-beam sculpting[79] have also been used for this purpose. Highlighted are the improvements reported by Meller's group on SiN nanopores approaching the effect of the salt gradients.[191] The same group[192] has also recently achieved the single-molecule detection of specific DNA sequences hybridizing double-stranded DNA (dsDNA) with peptide nucleic acid (PNA) probes and electrophoretically threading the DNA through sub-5 nm diameter SiN pores, opening up a wide range of possibilities in human genomics as well as in pathogen detection for fighting infectious diseases. Furthermore, nanoporous gold prepared by selective dissolution of silver from a silver/gold alloy has also been used to develop a DNA biosensor using multifunctional encoded DNA-Au bio-barcodes.[193]

In addition to the cylindrical ones, conical-shaped gold nanotubes have also been used for DNA analysis by Martin's group, achieving even mismatch selectivity,[194] and taking advantage of that geometry that offers a dramatic enhancement in the rate of transport through the membrane.

Finally, it deserves to be highlighted the very interesting work recently reported by Garaj *et al.*[195] related to the use of graphene membranes. They do electrical measurements on graphene membranes in which a single nanopore is drilled, showing that the membrane's effective insulating thickness is less than 1 nm. This small effective thickness makes graphene a suitable substrate for very high-resolution, high-throughput nanopore-based single-molecule detectors, being successfully applied here for the DNA sequencing. The important achievements reported in this work seem to indicate that graphene-based nanochannels offer new insights into atomic surface processes and sensor development opportunities.

Protein Detection. Cylindrical solid-state nanochannels are also capable of the label-free analysis of proteins. Of special interest is the very recent work reported by Wei *et al.*,[196] where the use of metallized silicon

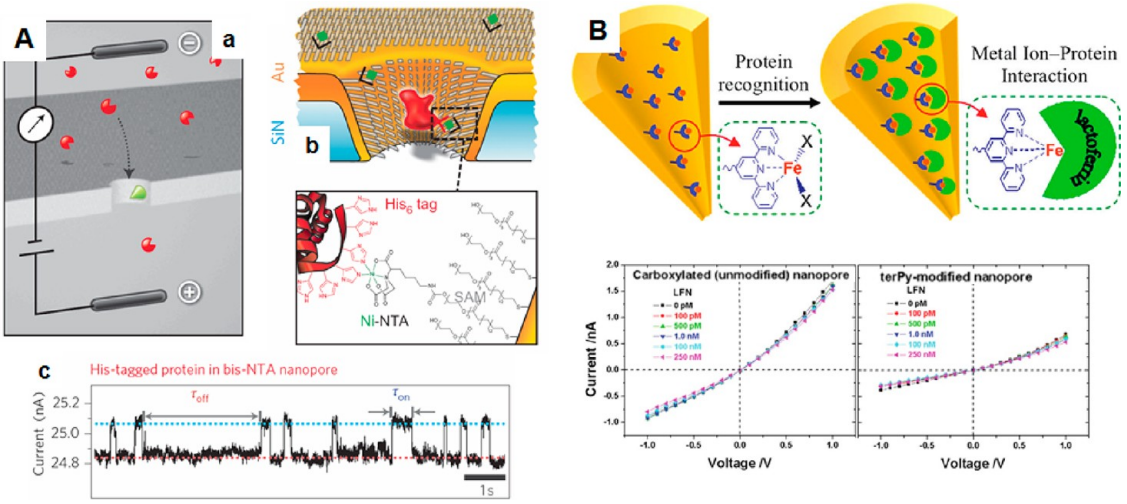

Figure 9. Protein sensing using chemically modified single solid-state nanochannels. (A) (a) Cross-sectional sketch depicting the principle of single-molecule sensing with a nanochannel: a membrane with a single nanochannel separates two electrolyte-filled compartments. Charged analyte molecules (red) are electrokinetically driven through the channel and are detected by transient blockades in the trans-channel ion current. When the channel is equipped with a specific receptor site (green), the blockade time reflects the binding time of the analyte (ligand) to the receptor. (b) Schematic cross section of a gold-coated SiN nanochannel functionalized with thiols and NTA receptor thiols. The Ni2p-loaded (green) nitrilotriacetic receptor (black) specifically binds His6-tagged proteins (red). (c) Representative current *versus* time trace signals. Adapted with permission from ref 196. Copyright 2012 Nature Publishing Group. (B) Schematic representation of a single conical nanochannel with covalently immobilized terpyridine ligand for lactoferrin detection, *via* the metal ion affinity-based biomolecular recognition, and graphs of the current *vs* voltage characteristics of a single conical nanochannel with before (left) and after (right) the covalent attachment of terpyridine, followed by the addition of various concentration of lactoferrin. Adapted from ref 202. Copyright 2011 American Chemical Society.

nitride nanopores chemically modified with nitrilotriacetic acid receptors for the stochastic sensing of proteins is described. The authors found that reversible binding and unbinding of the proteins to the receptors can be monitored in real time and also demonstrated the versatile nature of this approach for His-tagged protein detection (Figure 9A). These kinds of cylindrical-shaped solid-state single nanochannels in silicon nitride[197,198] and also in polymeric[199] membranes have also been used by other authors for the study of protein translocation.

On the other hand, conical-shaped nanochannels are ideally suited for resistive-pulse sensing applications, due to a focusing effect that makes ion current focused toward the electrolyte solution at the tip opening of the nanochannel. For this reason, ion current is extremely sensitive to analyte species present in the tip of these kinds of nanochannels. Thus, polymeric membranes have been used to generate these conical nanochannels by the track-etch method and applied for electrochemical detection of proteins.[183,200] Even single porphyrin molecules (a molecular analyte, opposed to a particle or macromolecule) have been sensed based on similar principles, using a conically shaped nanochannel prepared by the track-etch method as the sensing element as done by Martin's group.[201] They sensed the molecular analyte due to the small diameter opening of the conical nanochannel (up to 4.5 nm), which is comparable to the diameter of the analyte molecule (*i.e.*, porphyrin, which is up to 2 nm). Furthermore, conical nanochannels in polymeric membranes modified with metal-chelating ligands have been used for the detection of proteins such as lactoferrin, *via* the metal ion affinity-based biomolecular recognition[202] (Figure 9B).

Finally, conical gold nanotubes embedded within polymeric membranes have also been used, to a minor extent, for protein detection.[203]

Other Analyte Sensing. In addition to the extensive use of solid-state single nanochannles in DNA and protein detection, other interesting applications of these sensing systems have been reported in the past years. This is the case of the biomimetic potassium responsive nanochannel closely imitating the *in vivo* condition recently developed by Hou *et al.*,[204] immobilizing G-quadruplex DNA onto a synthetic nanochannel embedded in a track-etched polyethylene terephthalate membrane, undergoing a potassium responsive conformational change and then inducing a change in the effective pore size (Figure 10A). Another very recent interesting application that deserves to be highlighted is the possibility of using resistive-pulse sensors for electrokinetic surface charge measurements of nanoparticles.[205] It can be done by using flexible polyurethane membranes containing single conical nanochannels and recording the particle blockade rate for different pressures applied across a pore sensor, due to the combination of the applied pressure with electro-osmosis and electrophoresis effects (Figure 10B).

Finally, we consider it relevant to highlight the work done by White and co-workers,[206,207] who described

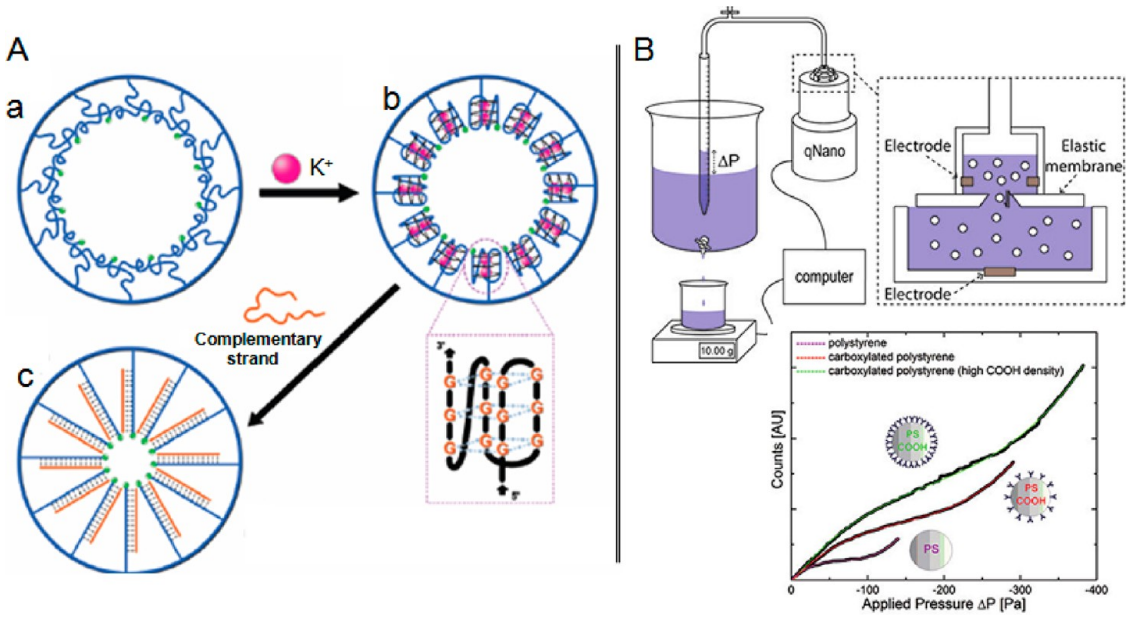

Figure 10. Other analytes sensing with solid-state nanochannels. (A) Biomimetic potassium responsive nanochannel: (a) G4 DNA is immobilized onto the inner surface of a single nanochannel. In the absence of K^+, the G4 DNA relaxes to a loosely packed single-stranded structure. (b) In the presence of K^+, the G4 DNA folds into densely packed rigid quadruplex structures that partially decrease the effective nanochannel diameter. (c) After adding cDNA strands, G4 DNA forms a closely packed arrangement of double-stranded DNA on the single nanochannel. Adapted from ref 204. Copyright 2009 American Chemical Society. (B) Characterization of nanoparticle surface charge: pressure in the top fluid cell is controlled *via* a flexible tubing connection by varying the height difference between the water level in a partially submerged buret and the water level of a large water reservoir. The buret is equilibrated with atmospheric pressure by opening a valve. The graph represents S-curves obtained for various polystyrene particles, acquired using the variable pressure method. Adapted from ref 205. Copyright 2012 American Chemical Society.

the fabrication and electrochemical behavior of conical-shaped glass nanopore electrodes not only as platforms for investigating molecular transport through orifices of nanoscale dimensions but also as sensors after chemical modification. Furthermore, they also found that the cone-shaped glass nanopore structures were ideal for containing additional functional layers, such as ion-selective membranes. After these pioneering works, they reported a novel glass nanopore-based ion-selective electrode (ISE) for the detection of Cl^- ions in scanning electrochemical microscope experiments to map the ion flux through a micropore.[208] They fabricated the all-solid-state ISE by sealing a conically etched platinum wire into a soda lime glass capillary and created the conical nanopore after polishing. Then they electroplated Ag on the Pt electrode in the pore and chlorinated to obtain a Ag/AgCl layer within the pore, resulting in a Ag/AgCl layer-coated ISE highly selective to Cl^-.

Use of Solid-State Nanochannel Arrays. DNA Analysis. Recent works are focused on the use of arrays of nanochannels as modifiers of conventional electrotransducer surfaces and measuring the changes of the electrochemical response of an electroactive species in solution due to the presence of the analyte inside the channels. Al_2O_3 membranes prepared by anodization have a high pore density ($1 \times 10^9/cm^2$) and small pore diameters, which results in a substrate with high surface area that can be easily functionalized and very advantageous for biosensing. These characteristics, together with their commercial availability, have made them one of the preferred nanoporous substrates for biosensing applications. For example, hydroxyl groups on the Al_2O_3 surface can be used for chemical functionalization and join to amino groups of 5′-aminated DNA. This approach can be applied for DNA detection and separation. The surface charge effect in controlling ionic conductance through a nanoporous Al_2O_3 membrane has also been investigated by Smirnov's group for its application in the detection of unlabeled DNA.[209] For example, nanoporous Al_2O_3 modified with covalently linked DNA has been used to detect target DNA by monitoring the increase in impedance at the electrode upon DNA hybridization, which results from blocking the channels to ionic flow.[84] Cyclic voltammetry, direct current conductance, impedance spectroscopy, and even electrical impedance[210] were the electrochemical techniques tested, and $Fe(CN)_6^{4-/3-}$ and $Ru(NH_3)_6^{2+/3+}$ were the redox pairs used to probe the efficiency of ion blockage. After the covalent immobilization of the DNA probe inside the chemically modified nanochannels, the hybridization of target DNA takes place. For the electrical measurements, the back layer of aluminum under the membrane acts as working electrode and a polished aluminum rod as the counter electrode

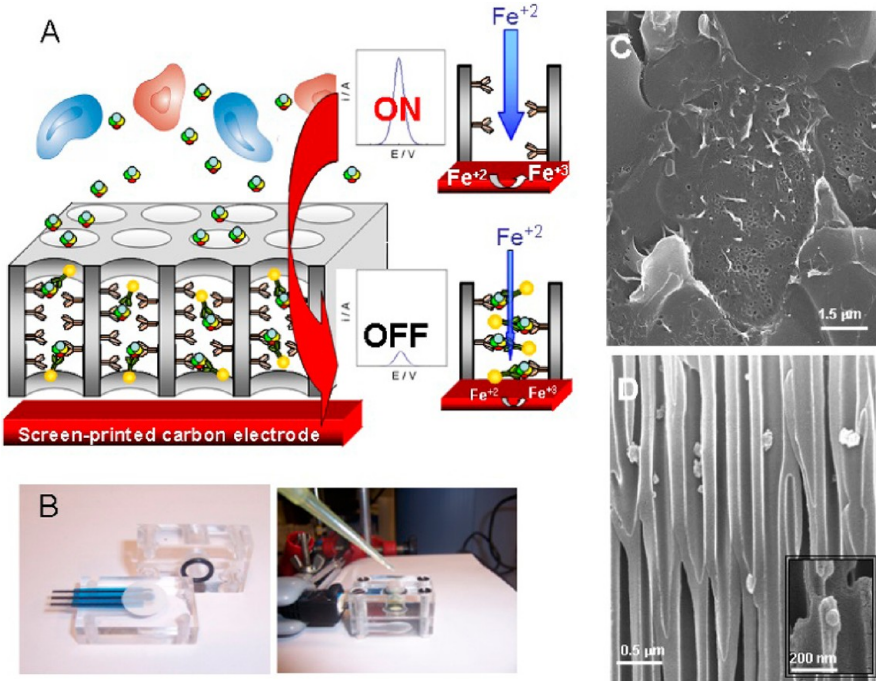

Figure 11. Protein sensing technology using an anodized aluminum oxide (AAO) nanoporous membrane array and AuNP labels. (A) Matrix interferents in the blood sample (cells or other material) remain outside of the channels, and the proteins enter inside and are recognized by specific antibodies (left) generating a blockage in the diffusion of electroactive species (Fe^{2+}) that can be enhanced using AuNP labels in a sandwich assay (right). (B) Electrochemical cell setup. (C) Top view of an AAO membrane on which a drop of blood (50 μL) was deposited. (D) Cross-sectional view of the same membrane after an immunoreaction using AuNP labels and silver enhancement (white silver crystals are observed). Adapted with permission from ref 214 (Copyright 2010 Science Direct) and ref 215 (Copyright 2011 Wiley).

immersed in electrolyte solution above the membrane. The hybridization causes an increase in the electrical impedance in KCl solution by more than 50%, with this change being related to the biological event. The effect of both electrostatic and steric effects of the DNA duplex on the diffusion of electroactive species in similar approaches has recently been thoroughly studied.[211]

Our group has recently reported a novel device and methodology for the rapid and simple label-free electrochemical detection of ssDNA using screen-printed carbon electrodes (SPCEs) modified with nanoporous Al_2O_3 membranes.[212] The membranes are functionalized with probe ssDNA, followed by the hybridization event that gives rise to the channel blocking. It was found that the blockage inside the nanochannels is fast and easy to detect by measuring the decrease in the differential pulse voltammetric (DPV) peak current of the $Fe(CN)_6^{4-/3-}$ redox species used as an indicator (Figure 11A,B). Although one of the main advantages of the nanochannel-based electrochemical sensing is that they are label-free systems, sometimes the limits of detection achieved are not enough to ensure their further application for the detection of analytes in real samples. In this context, our group has also demonstrated that the use of 20 nm gold nanoparticle (AuNP) tags increases the blockage inside the nanochannels, improving in this way the sensitivity of the assay. For the use of nanoparticles as analytical tools in nanochannel array sensing systems, the studies performed by White's group[213] related to the nanoparticle transport in nanochannels must be carefully considered, where it is concluded that nanoparticle size can be differentiated based on pulse height, and to a lesser extent based on translocation time.

Protein Detection. The same principles of the DNA hybridization detection based on the blockage of the diffusion of electroactive species through the mentioned Al_2O_3 membranes to the SPCEs have been recently approached by our group for the rapid and simple label-free electrochemical detection of human IgG as a model protein.[214] Furthermore, AuNPs were used as labels, and also, silver catalytic deposition on the AuNP labels was approached in order to obtain a higher blockage of the channels and improve the detection limits. The final optimized setup was applied for the detection of a breast cancer biomarker (CA15-3 protein) spiked in human blood samples, achieving clinical relevant detection limits and demonstrating a "dual" character of the membranes: as sensing platforms and also as "filters" minimizing matrix interferences due to size-exclusion effects (Figure 11C).[215] A similar approach has been very recently reported using aptamers as bioreceptors for the detection of thrombin in blood.[216] This nanochannel/nanoparticle biosensing system would have enormous potential in future miniaturized designs adapted to mass production technologies such as screen-printing technology.

In addition to the Al_2O_3 membranes, other arrays of synthetic nanochannels have been used, to a minor extent, for protein sensing. This is the case of the ion channel biosensors constructed onto the surface of gold-coated quartz crystal electrodes by Hou *et al.*[217] They immobilized on a gold electrode a positively charged metallopeptide which mimicked the section of a viral transmembrane glycoprotein with its pocket that is suitable for the binding of small molecules. The resulting sensor consequently acts as an artificial ion channel. The voltammetric signal of the $Fe(CN)_6^{4-/3-}$ system is modulated by specific analyte binding to the coiled coil. The results indicate that nanomolar quantities of peptides and small molecules that bind in the hydrophobic pocket could be selectively detected, providing a method for label-free detection of binding to a viral transmembrane glycoprotein and opening promising perspectives

Optical-Based Biosensing Applications. In addition to the extensive use in electroanalysis, powerful optical tools such as fluorescence, interferometry, and photonics have been reported in the last years as reading techniques in nanochannel array-based sensors. In addition to the possibility of detecting optical labels, some nanoporous materials possess optical properties that can change during the presence of specific analytes in the inner walls of the nanochannels in label-free assays. The use of single nanochannels has not been extensively reported here, so it will not be considered in this review.

Consequently, in spite of the fact that the inherent drawbacks of the optical detection techniques (time and cost of analysis and necessity of labels in some cases), which have limited the implementation of these sensing systems compared to the electrical-based ones, attention should be directed to some recent interesting approaches that could open new perspectives in this field.

Fluorescence and Photoluminescence Detection. The most common fluorescence-based biosensing approaches are focused on the detection of DNA, taking advantage of the use of Al_2O_3 membranes and fluorescent dyes. A representative example of a flow-through-type DNA array fabricated by fixing a single-stranded probe DNA to the inner walls of holes in an ideally ordered anodic porous Al_2O_3 substrate coated with a platinum layer was reported by Matsumoto *et al.*[218] They allowed the target DNA to flow through the holes, and the DNA hybridization reaction gave rise to discrete, ordered spots of fluorescence emitted from each nanometer-scale hole. Porous Al_2O_3 was also employed by Ma *et al.*[219] as a model chromatographic packing material for the depth-resolved fluorescence imaging recording of the real-time motion of single DNA molecules at the liquid/solid interface. They found that the residence time and the number of immobilized DNA molecules were higher when the pore size was larger and the pore diameter must be significantly

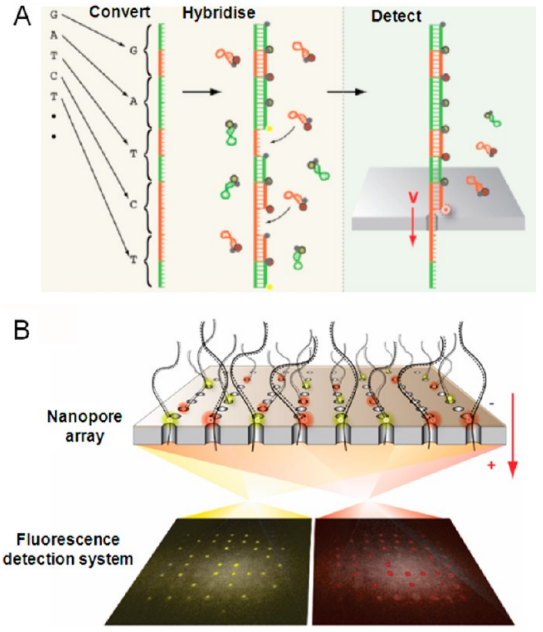

Figure 12. Simultaneous multiple optical DNA sequencing. (A) Bulk biochemical conversion of each nucleotide of the target DNA sequence to a known oligonuclotide, followed by hybridization with molecular beacons. Threading of the DNA/beacon complex through a nanochannel allows optical detection of the target DNA sequence. (B) Schematic illustration of the conceptual parallel readout scheme. Adapted from ref 221. Copyright 2010 American Chemical Society.

larger than the DNA short radius in order to allow the DNA capture. These achievements opened new perspectives in the field of conventional liquid chromatography as well as in the size-exclusion chromatography and membrane separations.

Kim *et al.*[220] also patterned a nanoporous Al_2O_3 membrane for the extraction of DNA from multiple samples simultaneously using multiple wells. They successfully observed DNA, labeled with a fluorescent marker, collected on the membrane, opening very interesting perspectives for further application in lab-on-a-chip-type systems that include DNA extraction steps.

Outstanding is the work reported by Meller's group,[221] using arrays of nanochannels generated in this case in SiN membranes by electron-beam lithography for the optical single-molecule DNA sequencing, employing a novel and ingenious multicolor readout. They first converted target DNA according to a binary code: each nucleotide of the target DNA sequence was biochemically converted in bulk to a known oligonucleotide. After that, they performed the hybridization with molecular beacons (with two types of fluorophores) and finally optically detected the target DNA by threading the DNA/beacon complex through the nanochannel. Furthermore, they used the array of nanochannels to sequentially strip off the beacons and, due to the specific location of each pore in the visual field of the optical detector, they achieved the simultaneous readout of the array (Figure 12).

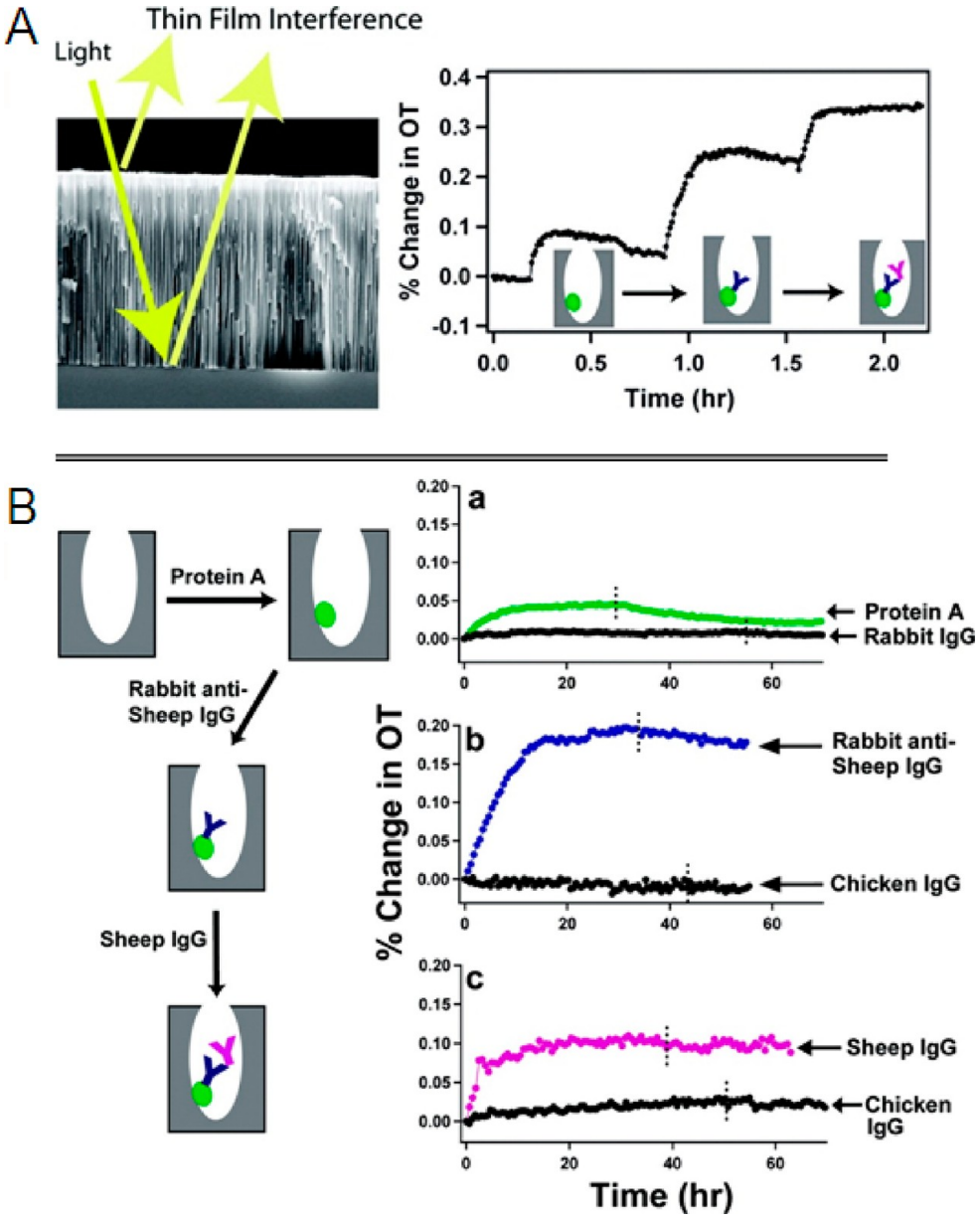

Figure 13. Label-free interferometric immunosensor. (A) Sensing principle: white light reflection from the porous aluminum oxide films generates a thin film interference spectral pattern that changes as a result of the modification in refractive index of the film generated by the immunoreaction. (B) Experiments demonstrating specific binding affinity and controls for the interferometric immunosensor. Adapted from ref 225. Copyright 2009 American Chemical Society.

Finally, intrinsic photoluminescence properties of nanoporous Al_2O_3 membranes have very recently been explored by Marsal's group,[222] and the characteristic barcode signals obtained could open the way for future applications in "smart" biosensors.

Interferometric Detection. Porous thin films also have the ability of increasing the sensitivity of interferometric sensors.[223] The principle of a porous thin film interferometer consists of the measurement of a change in the average index of refraction (η) of a fixed thickness layer (L). Analyte binding in the inner walls of the nanochannel gives rise to a change in the refractive index throughout the film and therefore to a change in the value of ηL.[224] With regard to this property, we note the label-free interferometric immunosensor on porous alumina membranes recently reported by Álvarez *et al.*[225] They immobilized antibodies inside the walls of the channels of an Al_2O_3 membrane through protein A binding and detected the specific immunoreaction with IgG by measuring the changes in the interferometric response (Figure 13). However, inherent limitations of this technique, such as nonlinearity in the output signal of the sensor, difficulty distinction of strain direction, and the requirement of complex fringe counting techniques, have minimized their use for biosensing on nanoporous materials.

Photonic Detection on Porous Silicon. The science of photonics includes the generation, emission, transmission,

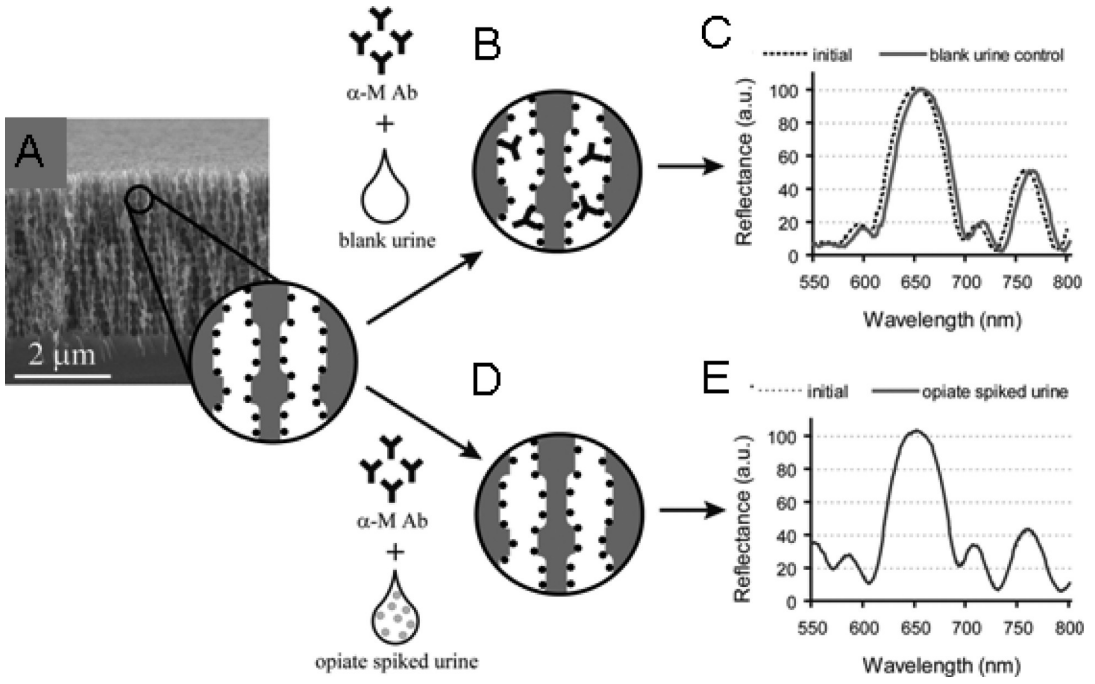

Figure 14. Photonic sensor on porous silicon (PSi). (A) Cross-sectional SEM of PSi Bragg mirror architecture. Inset depicts schematic of an opiate analogue functionalized PSi. (B) In the absence of free drug in urine, maximum Ab binds to surface-attached opiate analogue resulting in (C) a maximum wavelength shift response. (D) Opiates in urine compete with surface-attached opiate analogue for Ab binding sites, resulting in a proportional decrease in the wavelength shift response (*E*). Adapted from ref 230. Copyright 2010 American Chemical Society.

modulation, signal processing, switching, amplification, detection, and sensing of light using photons (both particle and light nature), covering all technical applications of light over the whole spectrum from ultraviolet over the visible to the near-, mid-, and far-infrared. However, in spite of this wide potential, most of the reported applications are in the range of the visible and near-infrared light.

Porous silicon (PSi) is an attractive porous material for biological and other applications due to the easy manipulation of their pore size, surface chemistry, and optical properties. For example, by tuning the current density, waveform, and solution composition used during the electrochemical etch, parameters such as the position, width, and intensity of spectral reflectivity peaks can be controlled. This allows the preparation of multilayered PSi (so-called PSi photonic crystals) which can display any number of colors within the visible spectrum, so PSi polytype quasi-regular structures with many interesting properties can be easily obtained.

In recent years, PSi photonic crystals have been used as biosensor platforms.[130,226−229] These multilayered PSi-based biosensors offer many of the advantages both PSi materials and photonic crystal sensors: large surface area, easy preparation, label-free possibilities, and compatibility with standard microelectronics processing. We also would like to highlight the work reported by DeLouise's group,[230] where the label-free detection of a broad range of opiates is achieved. They determined the wavelength shift sensitivity by tracking the infiltration of liquids with known refractive index (η) values and measured the reflectance spectra normal to the surface using a spectrophotometer after exposing the PSi sensor to a normal incident beam of white light (Figure 14).

However, in spite of these promising results, many external random factors produced from the electrochemical process in the fabrication of a PSi photonic crystal have a great influence on the fabrication of accurate ones, limiting the commercial application of PSi photonic crystal-based sensors.

CONCLUSIONS AND PROSPECTS

Nanochannels are proving to be an interesting platform for biosensing applications. This significant growth of interest in nanoporous materials has started from the platforms used for sensing designs with electrochemical detection, mimicking the processes that occur in natural ion channels and taking advantage of the inherent properties of the electrochemical techniques. Since maintaining a natural environment in an artificial device is a difficult task, the construction of fully and highly functional artificial systems with the ability of mimicking natural systems is demanded. This challenging subject led to the creation of different strategies to obtain artificial structures resembling the characteristics of ion channels commonly encountered in the membranes of living systems. In most cases, polymeric membranes are used as substrate material to generate nanochannels.

TABLE 1. Summary of the Various Nanopores/Nanochannels Used for Biosensing Applications

nanopore/nanochannel	single/array	material/fabrication	detection	analyte	ref
biological ion channel	single	α-hemolysin pore	electrical/stochastic sensing	DNA	51−55
				proteins	50, 57−59
				enzymes	60, 61
				peptides	62−64
				other analytes	49, 65
				DNA (sequencing perspectives)	21, 66−68, 71
	array	α-hemolysin pore	electrical/stochastic sensing	DNA	74
solid-state nanochannel	single	SiN-SiO_2 membranes/EBL[a]-FIB[a]	electrical/stochastic sensing	DNA	185−189, 191, 192
				proteins	197, 198
		Al_2O_3 membranes/EBL-FIB	electrical/stochastic sensing	DNA	79, 190
		polymeric membranes/ETCH[a]	electrical/stochastic sensing	proteins	183, 199−203
				other analytes	204, 205
		glass nanopore electrode	electrical/stochastic sensing	ions	206−208
	array	Al_2O_3 membranes/anodization	electrical/electrode blockage	DNA	209−212
				proteins	214−216
			optical/fluorescent labels	DNA	218−220
			interferometric	proteins	225
		SiN membranes/EBL	optical/fluorescent labels	DNA	221
		porous silicon/anodization	photonic−interferometric	proteins	130, 226, 228
				other analytes	227, 229, 230

[a] EBL, electron-beam lithography; FIB, focused ion beam; ETCH, track-etch method.

The typical experimental setup consists of measuring the changes in the electrical conductance between both sides of the membrane where a single nanochannel is inserted, inspired by the Coulter counter device. In this way, many works reporting DNA detection using both biological and solid-state nanochannels have been published in the last years, as summarized in Table 1. To a lower extent, proteins and other analytes have also been electrochemically analyzed based on the same fundament. As also evidenced in the table, from the wide range of materials and methods available, single solid-state nanochannels prepared from silicon nitride/oxide membranes by taking advantage of the electron-beam lithography and especially of the recent advances in ion-beam sculpting, together with those prepared from polymeric membranes by the track-etch method, have been shown as the most adequate for this kind of sensing. The main advantages of this kind of single nanochannel-based electrochemical sensing can be summarized as follows: (i) high sensitivity; (ii) rapid and reversible response (allowing real-time monitoring); (iii) wide dynamic range; (iv) several analytes can be quantified concurrently by a single sensing element; (v) the sensing element need not to be highly selective, as each analyte produces a characteristic signature; (vi) fouling of the sensing element cannot give a false reading, as the signal would not be characteristic of an analyte; and (vii) potential for nanoscale miniaturization.

Furthermore, in the case of the biological ion channels, the most exciting perspectives are focused on their integration in artificial substrates (hybrid biological/solid-state nanochannels) and the potential ability for DNA sequencing, as recently demonstrated and even commercialized by some companies.

The dream of a multianalyte sensing system with arrays of nanochannels is still far from being accomplished, due to the difficulty of adapting the Coulter counter concept to a multi-reading system. However, the use of arrays of solid-state nanochannels has opened the way to different and versatile sensing systems, mainly based on the blockage of electrotransducer surfaces. Here, Al_2O_3 nanoporous membranes prepared by anodization of the aluminum metal substrate are the most used materials, due to their advantageous properties and mass production opportunities. These nanoporous membranes have been shown to be excellent platforms for the analysis of real samples of, for example, human blood, due to their filtering properties, allowing minimization of matrix effects. Furthermore, these nanoporous membranes possess optical properties, which allows the sensitive analysis of a variety of analytes using powerful optical techniques such as interferometry or photonics-based ones, in the last case taking advantage of the photonic crystals prepared from porous silicon.

These entire advantages make the nanochannel-based biosensing systems a very promising research area that should bring wonderful scientific discoveries, with tremendous potential applications in fields such as diagnostics, safety-security, and other industrial applications. Nanochannel-based biosensing technologies would take advantages from the recent developments of nanoimprinting technologies (*i.e.*, roll-to-roll printing) that together with other fabrication techniques and emerging nanomaterials may bring new opportunities in terms of robustness, mass production,

and better tailoring of nanochannel-based platforms toward various applications delivering this advantageous technology to more users interested in protein, DNA, and cell sensing.

Conflict of Interest: The authors declare no competing financial interest.

Acknowledgment. The authors would like to acknowledge MEC (Madrid) for the project MAT2011-25870 and E.U.'s support under FP7 contract number 246513 "NADINE".

REFERENCES AND NOTES

1. Erickson, J. S.; Ligler, F. S. Analytical Chemistry: Home Diagnostics to Music. *Nature* **2008**, *456*, 178–179.
2. Ronkainen, N. J.; Halsall, H. B.; Heineman, W. R. Electrochemical Biosensors. *Chem. Soc. Rev.* **2010**, *39*, 1747–1763.
3. Merkoçi, A. Nanoparticles-Based Strategies for DNA, Protein and Cell Sensors. *Biosens. Bioelectron.* **2010**, *26*, 1164–1177.
4. de la Escosura-Muñiz, A.; Parolo, C.; Merkoçi, A. Immunosensing Using Nanoparticles. *Mater. Today* **2010**, *13*, 24–34.
5. de la Escosura-Muñiz, A.; Ambrosi, A.; Merkoçi, A. Electrochemical Analysis with Nanoparticle-Based Biosystems. *Trends Anal. Chem* **2008**, *27*, 568–584.
6. Merkoçi, A.; Pumera, M.; Llopis, X.; Pérez, B.; Del Valle, M.; Alegret, S. New Materials for Electrochemical Sensing VI: Carbon Nanotubes. *Trends Anal. Chem* **2005**, *24*, 826–838.
7. Aragay, G.; Pons, J.; Merkoçi, A. Recent Trends in Macro-, Micro-, and Nanomaterial-Based Tools and Strategies for Heavy-Metal Detection. *Chem. Rev.* **2011**, *111*, 3433–3458.
8. Coulter, W. H. Means for Counting Particles Suspended in a Fluid. U.S. Patent No. 2,656,508, 1953.
9. Coulter, W. H. High Speed Automatic Blood Cell Counter and Cell Size Analyzer. *Proc. Natl. Electronics Conf.* **1956**, *12*, 1034.
10. Bezrukov, S. M.; Vodyanoy, I.; Parsegian, V. A. Counting Polymers Moving through a Single-Ion Channel. *Nature* **1994**, *370*, 279–281.
11. Vercoutere, W. A.; Winters-Hilt, S.; DeGuzman, V. S.; Deamer, D.; Ridino, S. E.; Rodgers, J. T.; Olsen, H. E.; Marziali, A.; Akeson, M. Discrimination Among Individual Watson–Crick Base Pairs at the Termini of Single DNA Hairpin Molecules. *Nucleic Acids Res.* **2003**, *31*, 1311–1318.
12. Albrecht, T.; Edel, J. B.; Winterhalter, M. New Developments in Nanopore Research: From Fundamentals to Applications. *J. Phys.: Condens. Matter* **2010**, *22*, 450301.
13. Idley, D. J.; Stanfield, P. R. *Ion Channels: Molecules in Action*; Cambrige University Press: New York, 1996.
14. Sisson, A. L.; Shah, M. R.; Bhosale, S.; Matile, S. Synthetic Ion Channels and Pores (2004–2005). *Chem. Soc. Rev.* **2006**, *35*, 1269–1286.
15. Hou, X.; Guo, W.; Jiang, L. Biomimetic Smart Nanopores and Nanochannels. *Chem. Soc. Rev.* **2011**, *40*, 2385–2401.
16. Siwy, Z. S.; Howorka, S. Engineered Voltage-Responsive Nanopores. *Chem. Soc. Rev.* **2010**, *39*, 1115–1132.
17. Munch, E.; Launey, M. E.; Alsem, D. H.; Saiz, E.; Tomsia, A. P.; Ritchie, R. O. Tough, Bio-Inspired Hybrid Materials. *Science* **2008**, *322*, 1516–1520.
18. Lee, H.; Lee, B. P.; Messersmith, P. B. A Reversible Wet/Dry Adhesive Inspired by Mussels and Geckos. *Nature* **2007**, *448*, 338–341.
19. Hou, X.; Jiang, L. Learning from Nature: Building Bio-Inspired Smart Nanochannels. *ACS Nano* **2009**, *3*, 3339–3342.
20. Martin, C. R.; Siwy, Z. S. Learning Nature's Way: Biosensing with Synthetic Nanopores. *Science* **2007**, *317*, 231–332.
21. Kasianowicz, J. J.; Robertson, J. W. F.; Chan, E. R.; Reiner, J. E.; Stanford, V.M. Nanoscopic Porous Sensors. *Annu. Rev. Anal. Chem.* **2008**, *1*, 737–766.
22. Doyle, D. A.; Cabral, J. M.; Pfutzner, R. A.; Kuo, A. L.; Gulbis, J. M.; Cohen, S. L.; Chait, B. T.; MacKinnon, R. The Structure of the Potassium Channel: Molecular Basis of K^+ Conduction and Selectivity. *Science* **1998**, *280*, 69–77.
23. Song, L. Z.; Hobaugh, M. R.; Shustak, C.; Cheley, S.; Bayley, H.; Gouaux, J. E. Structure of Staphylococcal α-Hemolysin, a Heptameric Transmembrane Pore. *Science* **1996**, *274*, 1859–1866.
24. Nguyen, T. L. Three-Dimensional Model of the Pore Form of Anthrax Protective Antigen: Structure and Biological Implications. *J. Biomol. Struct. Dyn.* **2004**, *22*, 253–265.
25. Howorka, S.; Siwy, Z. Nanopore Analytics: Sensing of Single Molecules. *Chem. Soc. Rev.* **2009**, *38*, 2360–2384.
26. Bayley, H.; Jayasinghe, L. Functional Engineered Channels and Pores. *Mol. Membr. Biol.* **2004**, *21*, 209–220.
27. Lolicato, M.; Reina, S.; Messina, A.; Guarino, F.; Winterhalter, M.; Benz, R.; De Pinto, V. Generation of Artificial Channels by Multimerization of β-Strands from Natural Porin. *Biol. Chem.* **2011**, *392*, 617–624.
28. Butler, T. Z.; Pavlenok, M.; Derrington, I. M.; Niederweis, M.; Gundlach, J. H. Single-Molecule DNA Detection with an Engineered MspA Protein Nanopore. *Proc. Natl. Acad. Sci. U.S.A.* **2008**, *105*, 20647–20652.
29. Borisenko, V.; Lougheed, T.; Hesse, J.; Füreder-Kitzmüller, E.; Fertig, N.; Behrends, J. C.; Woolley, G. A.; Schültz, G. J. Simultaneous Optical and Electrical Recording of Single Gramicidin Channels. *Biophys. J.* **2003**, *84*, 612–622.
30. Armstrong, K. M.; Quigley, E. P.; Quigley, P.; Crumrine, D. S.; Cukierman, S. Covalently Linked Gramicidin Channels: Effects of Linker Hydrophobicity and Alkaline Metals on Different Stereoisomers. *Biophys. J.* **2001**, *80*, 1810–1818.
31. Mayer, M.; Semetey, V.; Gitlin, I.; Yang, J.; Whitesides, G. M. Using Ion Channel-Forming Peptides to Quantify Protein-Ligand Interactions. *J. Am. Chem. Soc.* **2008**, *130*, 1453–1465.
32. Montal, M.; Mueller, P. Formation of Bimolecular Membranes from Lipid Monolayers and a Study of Their Electrical Properties. *Proc. Natl. Acad. Sci. U.S.A.* **1972**, *69*, 3561–3566.
33. Holden, M. A.; Bayley, H. Direct Introduction of Single Protein Channels and Pores into Lipid Bilayers. *J. Am. Chem. Soc.* **2005**, *127*, 6502–6503.
34. Holden, M. A.; Jayasinghe, L.; Daltrop, O.; Mason, A.; Bayley, H. Direct Transfer of Membrane Proteins from Bacteria to Planar Bilayers for Rapid Screening by Single-Channel Recording. *Nat. Chem. Biol.* **2006**, *2*, 314–318.
35. Jeon, T. J.; Malmstadt, N.; Schmidt, J. J. Hydrogel-Encapsulated Lipid Membranes. *J. Am. Chem. Soc.* **2006**, *128*, 42–43.
36. Hromada, L. P.; Nablo, B. J.; Kasianowicz, J. J.; Gaitan, M. A.; DeVoe, D. L. Single Molecule Measurements within Individual Membrane-Bound Ion Channels Using a Polymer-Based Bilayer Lipid Membrane Chip. *Lab Chip* **2008**, *8*, 602–608.
37. Ratajska-Gadomska, B.; Gadomski, W. Water Structure in Nanopores of Agarose Gel by Raman Spectroscopy. *J. Chem. Phys.* **2004**, *121*, 12583–12588.
38. Atanasov, V.; Knorr, N.; Duran, R. S.; Ingebrandt, S.; Offenhausser, A.; Knoll, W.; Koper, I. Membrane on a Chip. A Functional Tethered Lipid Bilayer Membrane on Silicon Oxide Surfaces. *Biophys. J.* **2005**, *89*, 1780–1788.
39. Andersson, M.; Keizer, H. M.; Zhu, C.; Fine, D.; Dodabalapur, A.; Duran, R. S. Detection of Single Ion Channel Activity on a Chip Using Tethered Bilayer Membranes. *Langmuir* **2007**, *23*, 2924–2927.
40. Drexler, J.; Steinem, C. Pore-Suspending Lipid Bilayers on Porous Alumina Investigated by Electrical Impedance Spectroscopy. *J. Phys. Chem. B* **2003**, *107*, 11245–11254.
41. Deme, B.; Marchal, D. Polymer-Cushioned Lipid Bilayers in Porous Alumina. *Eur. Biophys. J.* **2005**, *34*, 170–179.
42. Morais-Cabral, J. H.; Zhou, Y.; MacKinnon, R. Energetic Optimization of Ion Conduction Rate by the K^+ Selectivity Filter. *Nature* **2001**, *414*, 37–42.

43. Jiang, Y.; Lee, A.; Chen, J.; Cadene, M.; Chait, B. T.; MacKinnon, R. Crystal Structure and Mechanism of a Calcium-Gated Potassium Channel. *Nature* **2002**, *417*, 515–522.
44. Perozo, E.; Cortes, D. M.; Sompornpisut, P.; Kloda, A.; Martinac, B. Open Channel Structure of MscL and the Gating Mechanism of Mechanosensitive Channels. *Nature* **2002**, *418*, 942–948.
45. Siwy, Z.; Kosińska, I. D.; Fuliński, A.; Martin, C. R. Asymmetric Diffusion through Synthetic Nanopores. *Phys. Rev. Lett.* **2005**, *94*, 048102-1–048102-4.
46. Sui, H.; Han, B. G.; Lee, J. K.; Walian, P.; Jap, B. K. Structural Basis of Water-Specific Transport through the AQP1 Water Channel. *Nature* **2001**, *414*, 872–878.
47. Dutzler, R.; Campbell, E. B.; Cadene, M.; Chait, B. T.; MacKinnon, R. X-ray Structure of a ClC Chloride Channel at 3.0 Å Reveals the Molecular Basis of Anion Selectivity. *Nature* **2002**, *415*, 287–294.
48. Bayley, H.; Cremer, P. S. Stochastic Sensors Inspired by Biology. *Nature* **2001**, *413*, 226–230.
49. Braha, O.; Walker, B.; Cheley, S.; Kasianowicz, J. J.; Song, L.; Gouaux, J. E.; Bayley, H. Designed Pores as Components for Biosensors. *Chem. Biol.* **1997**, *4*, 497–505.
50. Cheley, S.; Xie, H.; Bayley, H. A Genetically Encoded Pore for the Stochastic Detection of a Protein Kinase. *ChemBioChem* **2006**, *7*, 1923–1927.
51. Howorka, S.; Cheley, S.; Bayley, H. Sequence-Specific Detection of Individual DNA Strands Using Engineered Nanopores. *Nat. Biotechnol.* **2001**, *19*, 636–639.
52. Nakane, J.; Wiggin, M.; Marziali, A. A Nanosensor for Transmembrane Capture and Identification of Single Nucleic Acid Molecules. *Biophys. J.* **2004**, *87*, 615–621.
53. Stoddart, D.; Heron, A.; Mikhailova, E.; Maglia, G.; Bayley, H. Single-Nucleotide Discrimination in Immobilized DNA Oligonucleotides with a Biological Nanopore. *Proc. Natl. Acad. Sci. U.S.A.* **2009**, *106*, 7702–7707.
54. Purnell, R. F.; Schmidt, J. J. Discrimination of Single Base Substitutions in a DNA Strand Immobilized in a Biological Nanopore. *ACS Nano* **2009**, *3*, 2533–2538.
55. Wang, Y.; Zheng, D.; Tan, Q.; Wang, M. X.; Gu, L. Q. Nanopore-Based Detection of Circulating MicroRNAs in Lung Cancer Patients. *Nat. Nanotechnol.* **2011**, *6*, 668–674.
56. Movileanu, L.; Howorka, S.; Braha, O.; Bayley, H. Detecting Protein Analytes That Modulate Transmembrane Movement of a Polymer Chain within a Single Protein Pore. *Nat. Biotechnol.* **2000**, *18*, 1091–1095.
57. Howorka, S.; Nam, J.; Bayley, H.; Kahne, D. Stochastic Detection of Monovalent and Bivalent Protein−Ligand Interactions. *Angew. Chem., Int. Ed.* **2004**, *43*, 842–846.
58. Xie, H.; Braha, O.; Gu, L. Q.; Cheley, S.; Bayley, H. Single-Molecule Observation of the Catalytic Subunit of cAMP-Dependent Protein Kinase Binding to an Inhibitor Peptide. *Chem. Biol.* **2005**, *12*, 109–120.
59. Rotem, D.; Jayasinghe, L.; Salichou, M.; Bayley, H. Protein Detection by Nanopores Equipped with Aptamers. *J. Am. Chem. Soc.* **2012**, *134*, 2781–2787.
60. Hurt, N.; Wang, H.; Akeson, M.; Lieberman, K. R. Specific Nucleotide Binding and Rebinding to Individual DNA Polymerase Complexes Captured on a Nanopore. *J. Am. Chem. Soc.* **2009**, *131*, 3772–3778.
61. Gyarfas, B.; Olasagasti, F.; Benner, S.; Garalde, D.; Lieberman, K. R.; Akeson, M. Mapping the Position of DNA Polymerase-Bound DNA Templates in a Nanopore at 5 Å Resolution. *ACS Nano* **2009**, *3*, 1457–1466.
62. Stefureac, R.; Waldner, L.; Howard, P.; Lee, J. S. Nanopore Analysis of a Small 86-Residue Protein. *Small* **2008**, *4*, 59–63.
63. Movileanu, L.; Schmittschmitt, J. P.; Scholtz, J. M.; Bayley, H. Interactions of Peptides with a Protein Pore. *Biophys. J.* **2005**, *89*, 1030–1045.
64. Oukhaled, G.; Mathe, J.; Biance, A. L.; Bacri, L.; Betton, J. M.; Lairez, D.; Pelta, J.; Auvray, L. Unfolding of Proteins and Long Transient Conformations Detected by Single Nanopore Recording. *Phys. Rev. Lett.* **2007**, *98*, 158101.
65. Gu, L. Q.; Braha, O.; Conlan, S.; Cheley, S.; Bayley, H. Stochastic Sensing of Organic Analytes by a Pore-Forming Protein Containing a Molecular Adapter. *Nature* **1999**, *398*, 686–690.
66. Kasianowicz, J. J.; Brandin, E.; Branton, D.; Deamer, D. W. Characterization of Individual Polynucleotide Molecules Using a Membrane Channel. *Proc. Natl. Acad. Sci. U.S.A.* **1996**, *93*, 13770–13773.
67. Venkatesan, B. M.; Bashir, R. Nanopore Sensors for Nucleic Acid Analysis. *Nat. Nanotechnol.* **2011**, *6*, 615–624.
68. Branton, D.; Deamer, D. W.; Marziali, A.; Bayley, H.; Benner, S. A.; Butler, T.; Di Ventra, M.; Garaj, S.; Hibbs, A.; Huang, X. *et al.* The Potential and Challenges of Nanopore Sequencing. *Nat. Biotechnol.* **2008**, *26*, 1146–1153.
69. Schmidt, J. J. Stochastic Sensors. *J. Mater. Chem.* **2005**, *15*, 831–840.
70. Hou, X.; Guo, W.; Jiang, J. Biomimetic Smart Nanopores and Nanochannels. *Chem. Soc. Rev.* **2011**, *40*, 2385–2401.
71. Clarke, J.; Wu, H. C.; Jayasinghe, L.; Patel, A.; Reid, S.; Bayley, H. Continuous Base Identification for Single-Molecule Nanopore DNA Sequencing. *Nat. Nanotechnol.* **2009**, *4*, 265–270.
72. Stoddart, D.; Maglia, G.; Mikhailova, E.; Heron, A. J.; Bayley, H. Multiple Base-Recognition Sites in a Biological Nanopore: Two Heads Are Better than One. *Angew. Chem., Int. Ed.* **2009**, *48*, 1–5.
73. Munroe, D. J.; Harris, T. J. R. Third-Generation Sequencing Fireworks at Marco Island. *Nat. Biotechnol.* **2010**, *28*, 426–428.
74. Osaki, T.; Suzuki, H.; Le Pioufle, B.; Takeuchi, S. Multichannel Simultaneous Measurements of Single-Molecule Translocation in α-Hemolysin Nanopore Array. *Anal. Chem.* **2009**, *81*, 9866–9870.
75. Iqbal, S. M.; Akin, D.; Bashir, R. Solid-State Nanopore Channels with DNA Selectivity. *Nat. Nanotechnol.* **2007**, *2*, 243–248.
76. Jirage, K. B.; Hulteen, J. C.; Martin, C. R. Nanotubule-Based Molecular-Filtration Membranes. *Science* **1997**, *278*, 655–658.
77. Kalman, E. B.; Sudre, O.; Vlassiouk, I.; Siwy, Z. S. Control of Ionic Transport through Gated Single Conical Nanopores. *Anal. Bioanal. Chem.* **2009**, *394*, 413–419.
78. Hou, X.; Dong, H.; Zhu, D.; Jiang, L. Fabrication of Stable Single Nanochannels with Controllable Ionic Rectification. *Small* **2010**, *6*, 361–365.
79. Venkatesan, B. M.; Estrada, D.; Banerjee, S.; Jin, X.; Dorgan, V. E.; Bae, M. H.; Aluru, N. R.; Pop, E.; Bashir, R. Stacked Graphene-Al_2O_3 Nanopore Sensors for Sensitive Detection of DNA and DNA−Protein Complexes. *ACS Nano* **2012**, *6*, 441–450.
80. Choi, B. G.; Hong, J.; Park, Y. C.; Jung, D. H.; Hong, W. H.; Hammond, P. T.; Park, H. Innovative Polymer Nanocomposite Electrolytes: Nanoscale Manipulation of Ion Channels by Functionalized Graphenes. *ACS Nano* **2011**, *5*, 5167–5174.
81. Gyurcsányi, R. E. Chemically-Modified Nanopores for Sensing. *Trends Anal. Chem.* **2008**, *27*, 627–639.
82. Fleischer, R. L.; Price, P. B. Tracks of Charged Particles in High Polymers. *Science* **1963**, *140*, 1221–1222.
83. Vlassiouk, I.; Krasnoslobodtsev, A.; Smirnov, S.; Germann, M. 'Direct' Detection and Separation of DNA Using Nanoporous Alumina Filters. *Langmuir* **2004**, *20*, 9913–9915.
84. Vlassiouk, I.; Takmakov, P.; Smirnov, S. Sensing DNA Hybridization *via* Ionic Conductance through a Nanoporous Electrode. *Langmuir* **2005**, *21*, 4776–4778.
85. Lee, S. B.; Mitchell, D. T.; Trofin, L.; Nevanen, T. K.; Soderlund, H.; Martin, C. R. Antibody-Based Bio/Nanotube Membranes for Enantiomeric Drug Separations. *Science* **2002**, *296*, 2198–2200.
86. Wu, M. Y.; Krapf, D.; Zandbergen, M.; Zandbergen, H.; Batson, P. E. Formation of Nanopores in a SiN/SiO_2 Membrane with an Electron Beam. *Appl. Phys. Lett.* **2005**, *87*, 113106-1–113106-3.
87. Nozawa, K.; Osono, C.; Sugawara, M. The Voltammetric Performance of Interdigitated Electrodes with Different Electron-Transfer Rate Constants. *Sens. Actuators, B* **2007**, *126*, 632–640.

88. Apel, P. Y.; Korchev, Y. E.; Siwy, Z.; Spohr, R.; Yoshida, M. Diode-like Single-Ion Track Membrane Prepared by Electro-Stopping. *Nucl. Instrum. Methods Phys. Res., Sect. B* **2001**, *184*, 337–346.
89. Scopece, P.; Baker, L. A.; Ugo, P.; Martin, C. R. Conical Nanopore Membranes: Solvent Shaping of Nanopores. *Nanotechnology* **2006**, *17*, 3951–3956.
90. Dobrev, D.; Vetter, J.; Neumann, R.; Angert, N. Conical Etching and Electrochemical Metal Replication of Heavy-Ion Tracks in Polymer Foils. *J. Vac. Sci. Technol., B* **2001**, *19*, 1385–1387.
91. Li, N.; Yu, S.; Harrell, C. C.; Martin, C. R. Conical Nanopore Membranes. Preparation and Transport Properties. *Anal. Chem.* **2004**, *76*, 2025–2030.
92. Hou, X.; Zhang, H.; Jiang, L. Building Bio-Inspired Artificial Functional Nanochannels: From Symmetric to Asymmetric Modification. *Angew. Chem., Int. Ed.* **2012**, *51*, 5296–5307.
93. Storm, A. J.; Chen, J. H.; Ling, X. S.; Zandbergen, H. W.; Dekker, C. Fabrication of Solid-State Nanopores with Single-Nanometre Precision. *Nat. Mater.* **2003**, *2*, 537–540.
94. Li, J.; Stein, D.; McMullan, C.; Branton, D.; Aziz, M. J.; Golovchenko, J. A. Ion-Beam Sculpting at Nanometre Length Scales. *Nature* **2001**, *412*, 166–169.
95. Menard, L. D.; Ramsey, J. M. Fabrication of Sub-5 nm Nanochannels in Insulating Substrates Using Focused Ion Beam Milling. *Nano Lett.* **2011**, *11*, 512–517.
96. Cai, Q.; Ledden, B.; Krueger, E.; Golovchenko, J. A.; Li, J. Nanopore Sculpting with Noble Gas Ions. *J. Appl. Phys.* **2006**, *100*, 024914.
97. Schenkel, T.; Radmilovic, V.; Stach, E. A.; Park, S. J.; Persaud, A. Formation of a Few Nanometer-Wide Holes in Membranes with a Dual-Beam Focused Ion Beam System. *J. Vac. Sci. Technol., B* **2003**, *21*, 2720–2723.
98. Romano-Rodríguez, A.; Hernández-Ramírez, F. Dual-Beam Focused Ion Beam (FIB): A Prototyping Tool for Micro and Nanofabrication. *Microelectron. Eng.* **2007**, *84*, 789–792.
99. Bell, D. C.; Lemme, M. C.; Stern, L. A.; Marcus, C. M. Precision Material Modification and Patterning with He Ions. *J. Vac. Sci. Technol., B* **2009**, *27*, 2755–2758.
100. Zhang, B.; Zhang, Y.; White, H. S. The Nanopore Electrode. *Anal. Chem.* **2004**, *76*, 6229–6238.
101. Masuda, H.; Tanaka, H.; Baba, N. Preparation of Porous Material by Replacing Microstructure of Anodic Alumina Film with Metal. *Chem. Lett.* **1990**, *4*, 621–622.
102. Masuda, H.; Fukuda, K. Ordered Metal Nanohole Arrays Made by a Two-Step Replication of Honeycomb Structures of Anodic Alumina. *Science* **1995**, *268*, 1466–1468.
103. Foong, T. R. B.; Sellinger, A.; Hu, X. Origin of the Bottlenecks in Preparing Anodized Aluminum Oxide (AAO) Templates on ITO Glass. *ACS Nano* **2008**, *2*, 2250–2256.
104. Carporali, A.; Fossati, A.; Lavacchi, A.; Perissi, I.; Tolstogouzov, A.; Bardi, U. Aluminium Eletroplated from Ionic Liquids as Protective Coating Against Corrosion. *Corros. Sci.* **2008**, *50*, 534–539.
105. Liu, Q. X.; Abedin, Z. E.; Endres, F. Electroplating of Mild Steel by Aluminium in a First Generation Ionic Liquid: A Green Alternative to Commercial Al-Plating in Organic Solvents. *Surf. Coat. Technol.* **2006**, *201*, 1352–1356.
106. Hassel, A. W.; Bello-Rodriguez, B.; Milenkovic, S.; Schneider, A. Electrochemical Production of Nanopore Arrays in a Nickel Aluminium Alloy. *Electrochim. Acta* **2005**, *5*, 3033–3039.
107. Saleh, O. A.; Sohn, L. L. An Artificial Nanopore for Molecular Sensing. *Nano Lett.* **2003**, *3*, 37–38.
108. Cheng, J. Y.; Ross, C. A.; Smith, H. I.; Thomas, E. L. Templated Self-Assembly of Block Copolymers: Top-Down Helps Bottom-Up. *Adv. Mater.* **2006**, *18*, 2505–2521.
109. Lin, Y.; Boker, A.; He, J.; Sill, K.; Xiang, H.; Abetz, C.; Li, X.; Wang, J.; Emrick, T.; Long, S.; *et al.* Self-Directed Self-Assembly of Nanoparticle/Copolymer Mixtures. *Nature* **2005**, *434*, 55–59.
110. Park, S.; Kim, B.; Wang, J. Y.; Russell, T. P. Fabrication of Highly Ordered Silicon Oxide Dots and Stripes from Block Copolymer Thin Films. *Adv. Mater.* **2008**, *20*, 681–685.
111. Olson, D. A.; Chen, L.; Hillmyer, M. A. Templating Nanoporous Polymers with Ordered Block Copolymers. *Chem. Mater.* **2008**, *20*, 869–890.
112. Yang, S. Y.; Yang, J. A.; Kim, E. S.; Jeon, G.; Oh, E. J.; Choi, K. Y.; Hahn, S. K.; Kim, J. K. Single-File Diffusion of Protein Drugs through Cylindrical Nanochannels. *ACS Nano* **2010**, *4*, 3817–3822.
113. Chao, C. C.; Wang, T. C.; Ho, R. M.; Georgopanos, P.; Avgeropoulos, A.; Thomas, E. L. Robust Block Copolymer Mask for Nanopatterning Polymer Films. *ACS Nano* **2010**, *4*, 2088–2094.
114. Pokroy, B.; Epstein, A. K.; Persson-Gulda, M. C. M.; Aizenberg, J. Fabrication of Bioinspired Actuated Nanostructures with Arbitrary Geometry and Stiffness. *Adv. Mater.* **2009**, *21*, 463–469.
115. Lipomi, D. J.; Kats, M. A.; Kim, P.; Kang, S. H.; Aizenberg, J.; Capasso, F.; Whitesides, G. M. Fabrication and Replication of Arrays of Single- or Multicomponent Nanostructures by Replica Molding and Mechanical Sectioning. *ACS Nano* **2010**, *4*, 4017–4026.
116. Costner, E. A.; Lin, M. W.; Jen, W. L.; Willson, C. G. Nanoimprint Lithography Materials Development for Semiconductor Device Fabrication. *Annu. Rev. Mater. Res.* **2009**, *39*, 155–180.
117. Nakamoto, K.; Kurita, R.; Niwa, O. Electrochemical Surface Plasmon Resonance Measurement Based on Gold Nanohole Array Fabricated by Nanoimprinting Technique. *Anal. Chem.* **2012**, *84*, 3187–3191.
118. Yao, J.; Le, A. P.; Schulmerich, M. V.; Maria, J.; Lee, T. W.; Gray, S. K.; Bhargava, R.; Rogers, J. A.; Nuzzo, R. G. Soft Embossing of Nanoscale Optical and Plasmonic Structures in Glass. *ACS Nano* **2011**, *5*, 5763–5774.
119. Chanda, D.; Shigeta, K.; Gupta, S.; Cain, T.; Carlson, A.; Mihi, A.; Baca, A. J.; Bogart, G. R.; Braun, P.; Rogers, J. A. Large-Area Flexible 3D Optical Negative Index Metamaterial Formed by Nanotransfer Printing. *Nat. Nanotechnol.* **2011**, *6*, 402–407.
120. Walcarius, A.; Kuhn, A. Ordered Porous Thin Films in Electrochemical Analysis. *Trends Anal. Chem.* **2008**, *27*, 593–603.
121. Walcarius, A.; Sibottier, E.; Etienne, M.; Ghanbaja, J. Electrochemically Assisted Self-Assembly of Mesoporous Silica Thin Films. *Nat. Mater.* **2007**, *6*, 602–608.
122. Wan, Y.; Zhao, D. On the Controllable Soft-Templating Approach to Mesoporous Silicates. *Chem. Rev.* **2007**, *107*, 2821–2860.
123. Chang, H.; Joo, S. H.; Pak, C. Synthesis and Characterization of Mesoporous Carbon for Fuel Cell Applications. *J. Mater. Chem.* **2007**, *17*, 3078–3088.
124. Wang, X.; Xu, S.; Cong, M.; Li, H.; Gu, Y.; Xu, W. Hierarchical Structural Nanopore Arrays Fabricated by Pre-patterning Aluminum Using Nanosphere Lithography. *Small* **2012**, *8*, 972–976.
125. Bartlett, P. N.; Baumberg, J. J.; Birkin, P. R.; Ghanem, M. A.; Netti, M. C. Highly Ordered Macroporous Gold and Platinum Films Formed by Electrochemical Deposition through Templates Assembled from Submicron Diameter Monodisperse Polystyrene Spheres. *Chem. Mater.* **2002**, *14*, 2199–2208.
126. Reculusa, S.; Agricole, B.; Derre, A.; Couzi, M.; Sellier, E.; Delhaes, P.; Ravaine, S. Colloidal Crystals as Templates for Macroporous Carbon Electrodes of Controlled Thickness. *Electroanalysis* **2007**, *19*, 379–384.
127. Bartlett, P. N.; Birkin, P. R.; Ghanem, M. A.; Toh, C. S. Electrochemical Synthesis of Highly Ordered Macroporous Conducting Polymer Films Using Self-assembled Colloidal Templates. *J. Mater. Chem.* **2001**, *11*, 849–853.
128. Kuo, C. Y.; Huang, K. H.; Lu, S. Y. Fabrication of Synthetic Opals Composed of Mesoporous SnO_2 Spheres with an Anodization-Assisted Double Template Process. *Electrochem. Commun.* **2007**, *9*, 2867–2870.

129. Lee, J.; Kim, J.; Hyeon, T. Recent Progress in the Synthesis of Porous Carbon Materials. *Adv. Mater.* **2006**, *18*, 2073–2094.
130. Pacholski, C.; Sartor, M.; Sailor, M. J.; Cunin, F.; Miskelly, G. M. Biosensing Using Porous Silicon Double-Layer Interferometers: Reflective Interferometric Fourier Transform Spectroscopy. *J. Am. Chem. Soc.* **2005**, *127*, 11636–11645.
131. Snow, P. A.; Squire, E. K.; Russel, P.S. J.; Canham, L. T. Vapor Sensing Using the Optical Properties of Porous Silicon Bragg Mirrors. *J. Appl. Phys.* **1999**, *86*, 1781–1784.
132. Cunin, F.; Schmedake, T. A.; Link, J. R.; Li, Y. Y.; Koh, J.; Bhatia, S. N.; Sailor, M. J. Biomolecular Screening with Encoded Porous Silicon Photonic Crystals. *Nat. Mater.* **2002**, *1*, 39–41.
133. Ouyang, H.; Striemer, C. C.; Fauchet, P. M. Quantitative Analysis of the Sensitivity of Porous Silicon Optical Biosensors. *Appl. Phys. Lett.* **2006**, *88*, 163108.
134. Zhang, D. X.; Zhang, H. J. *In-Situ* Thickness Measurement of Porous Alumina by Atomic Force Microscopy and the Reflectance Wavelength Measurement from 400−1000 nm. *Microsc. Res. Tech.* **2006**, *69*, 267–270.
135. Rauf, A.; Mehmood, M.; Rasheed, M. A.; Aslam, M. The Effects of Ordering on the Morphology of Two-Layer Alumite-Forming a Patterned Interface. *Mater. Lett.* **2009**, *63*, 1601–1604.
136. Raimundo, D. S.; Caliope, P. B.; Huanca, D. R.; Salcedo, W. J. Anodic Porous Alumina Structural Characteristics Study Based on SEM Image Processing and Analysis. *Microelectron. J.* **2009**, *40*, 844–847.
137. Thompson, G. E.; Furneaux, R. C.; Wood, G. C.; Richardson, J. A.; Goode, J. S. Nucleation and Growth of Porous Anodic Films on Aluminium. *Nature* **1978**, *272*, 433–435.
138. Garcia-Vergara, S. J.; Skeldon, P.; Thompson, G. E.; Habazaki, H. Behaviour of a Fast Migrating Cation Species in Porous Anodic Alumina. *Corros. Sci.* **2008**, *50*, 3179–3184.
139. Zhu, Y. Y.; Ding, G. Q.; Ding, J. N.; Yuan, N. Y. AFM, SEM and TEM Studies on Porous Anodic Alumina. *Nanoscale Res. Lett.* **2010**, *5*, 725–734.
140. Banerjee, A.; Mikhailova, E.; Cheley, S.; Gu, L. Q.; Montoya, M.; Nagaoka, Y.; Gouaux, E.; Bayley, H. Molecular Bases of Cyclodextrin Adapter Interactions with Engineered Protein Nanopores. *Proc. Natl. Acad. Sci. U.S.A.* **2010**, *107*, 8165–8170.
141. Misakian, M.; Kasianowicz, J. J. Electrostatic Influence on Ion Transport through the α HL Channel. *J. Membr. Biol.* **2003**, *195*, 137–146.
142. Stoddart, D.; Heron, A. J.; Klingelhoefer, J.; Mikhailova, E.; Maglia, G.; Bayley, H. Nucleobase Recognition in ssDNA at the Central Constriction of the α-Hemolysin Pore. *Nano Lett.* **2010**, *10*, 3633–3637.
143. Bhattacharya, S.; Muzard, L.; Payet, L.; Mathé, J.; Bockelmann, U.; Aksimentiev, A.; Viasnoff, V. Rectification of the Current in α-Hemolysin Pore Depends on the Cation Type: The Alkali Series Probed by MD Simulations and Experiments. *J. Phys. Chem. C* **2011**, *115*, 4255–4264.
144. Liebes, Y.; Drozdov, M.; Avital, Y. Y.; Kauffmann, Y.; Rapaport, H.; Kaplan, W. D.; Ashkenasy, N. Reconstructing Solid State Nanopore Shape from Electrical Measurements. *Appl. Phys. Lett.* **2010**, *97*, 223105.
145. DeBlois, R. W.; Bean, C. P. Counting and Sizing of Submicron Particles by the Resistive Pulse Technique. *Rev. Sci. Instrum.* **1970**, *41*, 909–916.
146. Reyes, D. R.; Iossifidis, D.; Auroux, P. A.; Manz, A. Micro Total Analysis Systems. 1. Introduction, Theory, and Technology. *Anal. Chem.* **2002**, *74*, 2623–2636.
147. Lettmann, C.; Mockel, D.; Staude, E. Permeation and Tangential Flow Streaming Potential Measurements for Electrokinetic Characterization of Track-Etched Microfiltration Membranes. *J. Membr. Sci.* **1999**, *159*, 243–251.
148. Apel, P.; Schulz, A.; Spohr, R.; Trautmann, C.; Vutsadakis, V. Track Size and Track Structure in Polymer Irradiated by Heavy Ions. *Nucl. Instrum. Methods Phys. Res., Sect. B* **1998**, *146*, 468–474.
149. Yaroshchuk, A.; Zhukova, O.; Ulbricht, M.; Ribitsch, V. Electrochemical and Other Transport Properties of Nanoporous Track-Etched Membranes Studied by the Current Switch-Off Technique. *Langmuir* **2005**, *21*, 6872–6882.
150. Kirby, B. J.; Hasselbrink, E. F. The Zeta Potential of Microfluidic Substrates. 2. Data for Polymers. *Electrophoresis* **2004**, *25*, 187–202.
151. Yuan, Z.; García, A. L.; López, G. P.; Petsev, D. N. Electrokinetic Transport and Separations in Fluidic Nanochannels. *Electrophoresis* **2007**, *28*, 595–610.
152. Zhang, J.; Kamenev, A.; Shklovskii, B. I. Conductance of Ion Channels and Nanopores with Charged Walls. *Phys. Rev. Lett.* **2005**, *95*, 1481011–1481011.
153. Ito, T.; Audi, A. A.; Dible, G. P. Electrochemical Characterization of Recessed Nanodisk-Array Electrodes Prepared from Track-Etched Membranes. *Anal. Chem.* **2006**, *78*, 7048–7053.
154. Zhang, B.; Zhang, Y.; White, H. S. Steady-State Voltammetric Response of the Nanopore Electrode. *Anal. Chem.* **2006**, *78*, 477–483.
155. Perry, J. M.; Zhou, K.; Harms, Z. D.; Jacobson, S. C. Ion Transport in Nanofluidic Funnels. *ACS Nano* **2010**, *4*, 3897–3902.
156. Volkringer, C.; Popov, D.; Loiseau, T.; Guillou, N.; Ferey, G.; Haouas, M.; Taulelle, F.; Mellot-Draznieks, C.; Burghammer, M.; Riekel, C. A Microdiffraction Set-Up for Nanoporous Metal-Organic-Framework-Type Solids. *Nat. Mater.* **2007**, *6*, 760–764.
157. Pawsey, S.; Moudrakovski, I.; Ripmeester, J.; Wang, L. Q.; Exarhos, G. J.; Rowsell, J. L.; Yaghi, O. M. Hyperpolarized Xe-129 Nuclear Magnetic Resonance Studies of Isoreticular Metal-Organic Frameworks. *J. Phys. Chem. C* **2007**, *111*, 6060–6067.
158. Comotti, A.; Bracco, S.; Ferretti, L.; Valsesia, P.; Sozzani, P. 2D Multinuclear NMR, Hyperpolarized Xenon and Gas Storage in Organosilica Nanochannels with Crystalline Order in the Walls. *J. Am. Chem. Soc.* **2007**, *129*, 8566–8576.
159. Fyfe, C.; Brouwer, D. H. Optimization, Standardization, and Testing of a New NMR Method for the Determination of Zeolite Host−Organic Guest Crystal Structures. *J. Am. Chem. Soc.* **2006**, *128*, 11860–11871.
160. Baldus, M. Solid-State NMR: Molecular 3D Structure and Organization Seen at Atomic Level. *Angew. Chem., Int. Ed.* **2006**, *45*, 1186–1188.
161. Iuga, D.; Morais, C.; Gan, Z.; Neuville, D. R.; Cormier, L.; Massiot, D. NMR Heteronuclear Correlation between Quadrupolar Nuclei in Solids. *J. Am. Chem. Soc.* **2005**, *127*, 11540–11541.
162. Moudrakovski, I. L.; Nossov, A.; Lang, S.; Breeze, S. R.; Ratcliffe, C. I.; Simard, B.; Santyr, G.; Ripmeester, J. A. Continuous Flow NMR with Hyperpolarized Xenon for the Characterization of Materials and Processes. *Chem. Mater.* **2000**, *12*, 1181–1183.
163. Comotti, A.; Bracco, S.; Sozzani, P.; Horike, S.; Matsuda, R.; Chen, J.; Takata, M.; Kubota, Y.; Kitagawa, S. Nanochannels of Two Distinct Cross-Sections in a Porous Al-Based Coordination Polymer. *J. Am. Chem. Soc.* **2008**, *130*, 13664–13672.
164. Fritz, S. E.; Martin, S. M.; Frisbie, C. D.; Ward, M. D.; Toney, M. F. Structural Characterization of a Pentacene Monolayer on an Amorphous SiO_2 Substrate with Grazing Incidence X-ray Diffraction. *J. Am. Chem. Soc.* **2004**, *126*, 4084–4085.
165. Malachias, A.; Mei, Y.; Annabattula, R. K.; Deneke, C.; Onck, P. R.; Schmidt, O. G. Wrinkled-up Nanochannel Networks: Long-Range Ordering, Scalability, and X-ray Investigation. *ACS Nano* **2008**, *2*, 1715–1721.
166. Baklanov, M. R.; Mogilnikov, K. P.; Polovinkin, V. G.; Dultsev, F. N. Determination of Pore Size Distribution in Thin Films by Ellipsometric Porosimetry. *J. Vac. Sci. Technol., B* **2000**, *18*, 1385–1391.
167. Lee, H. J.; Soles, C. L.; Liu, D. W.; Bauer, B. J.; Wu, W. L. Pore Size Distributions in Low-k Dielectric Thin Films from X-ray Porosimetry. *J. Polym. Sci., Polym. Phys.* **2002**, *40*, 2170–2177.

168. Merkel, T. C.; Freeman, B. D.; Spontak, R. J.; He, Z.; Pinnau, I.; Meakin, P.; Hill, A. J. Ultrapermeable, Reverse-Selective Nanocomposite Membranes. *Science* **2002**, *296*, 519–522.
169. Shantarovich, V. P.; Azamatova, Z. K.; Novikov, Y. A.; Yampolskii, Y. P. Freevolume Distribution of High Permeability Membrane Materials Probed by Positron Annihilation. *Macromolecules* **1998**, *31*, 3963–3966.
170. Peng, H. G.; Vallery, R. S.; Liu, M.; Skalsey, M.; Gidley, D. W. Depth-Profiled Positronium Annihilation Lifetime Spectroscopy on Porous Films. *Colloids Surf., A* **2007**, *300*, 154–161.
171. Chen, C. C.; Derylo, M. A.; Baker, L. A. Measurement of Ion Currents through Porous Membranes with Scanning Ion Conductance Microscopy. *Anal. Chem.* **2009**, *81*, 4742–4751.
172. Pumera, M. Nanomaterials Meet Microfluidics. *Chem. Commun.* **2011**, *47*, 5671–5680.
173. Balasubramanian, K. Challenges in the Use of 1D Nanostructures for On-Chip Biosensing and Diagnostics: A Review. *Biosens. Bioelectron.* **2010**, *26*, 1195–1204.
174. Douville, N.; Huh, D.; Takayama, S. DNA Linearization through Confinement in Nanofluidic Channels. *Anal. Bioanal. Chem.* **2008**, *391*, 2395–2409.
175. Sordan, R.; Miranda, A.; Traversi, F.; Colombo, D.; Chrastina, D.; Isella, G.; Masserini, M.; Miglio, L.; Kern, K.; Balasubramanian, K. Vertical Arrays of Nanofluidic Channels Fabricated without Nanolithography. *Lab Chip* **2009**, *9*, 1556–1560.
176. Park, S.; Huh, Y. S.; Craighead, H. G.; Erickson, D. A Method for Nanofluidic Device Prototyping Using Elastomeric Collapse. *Proc. Natl. Acad. U.S.A.* **2009**, *106*, 15549–15554.
177. Utko, P.; Persson, F.; Kristensen, A.; Larsen, N. B. Injection Molded Nanofluidic Chips: Fabrication Method and Functional Tests Using Single-Molecule DNA Experiments. *Lab Chip* **2011**, *11*, 303–308.
178. Morais-Cabral, J. H.; Zhou, Y.; MacKinnon, R. Energetic Optimization of Ion Conduction Rate by the K^+ Selectivity Filter. *Nature* **2001**, *414*, 37–42.
179. Jiang, Y.; Lee, A.; Chen, J.; Cadene, M.; Chait, B. T.; MacKinnon, R. Crystal Structure and Mechanism of a Calcium-Gated Potassium Channel. *Nature* **2002**, *417*, 515–522.
180. Perozo, E.; Cortes, D. M.; Sompornpisut, P.; Kloda, A.; Martinac, B. Open Channel Structure of MscL and the Gating Mechanism of Mechanosensitive Channels. *Nature* **2002**, *418*, 942–948.
181. Siwy, Z.; Kosińska, I. D.; Fuliński, A.; Martin, C. R. Asymmetric Diffusion through Synthetic Nanopores. *Phys. Rev. Lett.* **2005**, *94*, 048102-1–048102-4.
182. Sui, H.; Han, B. G.; Lee, J. K.; Walian, P.; Jap, B. K. Structural Basis of Water-Specific Transport through the AQP1 Water Channel. *Nature* **2001**, *414*, 872–878.
183. Ali, M.; Yameen, B.; Neumann, R.; Ensinger, W.; Knoll, W.; Azzaroni, O. Biosensing and Supramolecular Bioconjugation in Single Conical Polymer Nanochannels. Facile Incorporation of Biorecognition Elements into Nanoconfined Geometries. *J. Am. Chem. Soc.* **2008**, *130*, 16351–16357.
184. Han, C. P.; Hou, X.; Zhang, H. C.; Guo, W.; Li, H. B.; Jiang, L. Enantioselective Recognition in Biomimetic Single Artificial Nanochannels. *J. Am. Chem. Soc.* **2011**, *133*, 7644–7647.
185. Chen, P.; Mitsui, T.; Farmer, D. B.; Golovchenko, J.; Gordon, R. G.; Branton, D. Atomic Layer Deposition To Fine-Tune the Surface Properties and Diameters of Fabricated Nanopores. *Nano Lett.* **2004**, *4*, 1333–1337.
186. Storm, A. J.; Storm, C.; Chen, J.; Zandbergen, H.; Joanny, J. F.; Dekker, C. Fast DNA Translocation through a Solid-State Nanopore. *Nano Lett.* **2005**, *5*, 1193–1197.
187. Ivanov, A. P.; Instuli, E.; Gilvery, C. M.; Baldwin, G.; Mc Comb, D. W.; Albrecht, T.; Edel, J. B. DNA Tunneling Detector Embedded in a Nanopore. *Nano Lett.* **2011**, *11*, 279–285.
188. Ayub, M.; Ivanov, A.; Hong, J.; Kuhn, P.; Instuli, E.; Edel, J. B.; Albrecht, T. Precise Electrochemical Fabrication of Sub-20 nm Solid-State Nanopores for Single-Molecule Biosensing. *J. Phys.: Condens. Matter* **2010**, *22*, 454128.
189. Storm, A. J.; Chen, J. H.; Zandbergen, H. W.; Dekker, C. Translocation of Double-Strand DNA through a Silicon Oxide Nanopore. *Phys. Rev. E* **2005**, *71*, 051903-1–051903-10.
190. Venkatesan, B. M.; Shah, A. B.; Zuo, J. M.; Bashir, R. DNA Sensing Using Nanocrystalline Surface-Enhanced Al_2O_3 Nanopore Sensors. *Adv. Funct. Mater.* **2010**, *20*, 1266–1275.
191. Wanunu, M.; Morrison, W.; Rabin, Y.; Grosberg, A. Y.; Meller, A. Electrostatic Focusing of Unlabelled DNA into Nanoscale Pores Using a Salt Gradient. *Nat. Nanotechnol.* **2010**, *5*, 160–165.
192. Singer, A.; Wanunu, M.; Morrison, W.; Kuhn, H.; Frank-Kamenetskii, M.; Meller, A. Nanopore Based Sequence Specific Detection of Duplex DNA for Genomic Profiling. *Nano Lett.* **2010**, *10*, 738–742.
193. Hu, K.; Lan, D.; Li, X.; Zhang, S. Electrochemical DNA Biosensor Based on Nanoporous Gold Electrode and Multifunctional Encoded DNA-Au Bio Bar Codes. *Anal. Chem.* **2008**, *80*, 9124–9130.
194. Kohli, P.; Harrell, C. C.; Cao, Z.; Gasparac, R.; Tan, W.; Martin, C. R. DNA-Functionalized Nanotube Membranes with Single-Base Mismatch Selectivity. *Science* **2004**, *305*, 984–985.
195. Garaj, S.; Hubbard, W.; Reina, A.; Kong, J.; Branton, D.; Golovchenko, J. A. Graphene as a Subnanometre Trans-Electrode Membrane. *Nature* **2010**, *467*, 190–194.
196. Wei, R.; Gatterdam, V.; Wieneke, R.; Tampe, R.; Rant, U. Stochastic Sensing of Proteins with Receptor-Modified Solid-State Nanopores. *Nat. Nanotechnol.* **2012**, *7*, 257–263.
197. Freedman, K. J.; Jürgens, M.; Prabhu, A.; Ahn, C. W.; Jemth, P.; Edel, J. B.; Kim, M. J. Chemical, Thermal, and Electric Field Induced Unfolding of Single Protein Molecules Studied Using Nanopores. *Anal. Chem.* **2011**, *83*, 5137–5144.
198. Talaga, D. S.; Li, J. Single-Molecule Protein Unfolding in Solid State Nanopores. *J. Am. Chem. Soc.* **2009**, *131*, 9287–9297.
199. Sexton, L. T.; Horne, L. P.; Sherrill, S. A.; Bishop, G. W.; Baker, L. A.; Martin, C. R. Resistive-Pulse Studies of Proteins and Protein/Antibody Complexes Using a Conical Nanotube Sensor. *J. Am. Chem. Soc.* **2007**, *129*, 13144–13152.
200. Wharton, J. E.; Jin, P.; Sexton, L. T.; Horne, L. P.; Sherrill, S. A.; Mino, W. K.; Martin, C. R. A Method for Reproducibly Preparing Synthetic Nanopores for Resistive-Pulse Biosensors. *Small* **2007**, *8*, 1424–1430.
201. Heins, E. A.; Siwy, Z. S.; Baker, L. A.; Martin, C. R. Detecting Single Porphyrin Molecules in a Conically Shaped Synthetic Nanopore. *Nano Lett.* **2005**, *5*, 1824–1829.
202. Ali, M.; Nasir, S.; Nguyen, Q. H.; Sahoo, J. K.; Tahir, M. N.; Tremel, W.; Ensinger, W. Metal Ion Affinity-Based Biomolecular Recognition and Conjugation Inside Synthetic Polymer Nanopores Modified with Iron Terpyridine Complexes. *J. Am. Chem. Soc.* **2011**, *133*, 17307–17314.
203. Siwy, Z.; Trofin, L.; Kohli, P.; Baker, L. A.; Trautmann, C.; Martin, C. R. Protein Biosensors Based on Biofunctionalized Conical Gold Nanotubes. *J. Am. Chem. Soc.* **2005**, *127*, 5000–5001.
204. Hou, X.; Guo, W.; Xia, F.; Nie, F. Q.; Dong, H.; Tian, Y.; Wen, L.; Wang, L.; Cao, L.; Yang, Y.; *et al.* A Biomimetic Potassium Responsive Nanochannel: G-Quadruplex DNA Conformational Switching in a Synthetic Nanopore. *J. Am. Chem. Soc.* **2009**, *131*, 7800–7805.
205. Vogel, R.; Anderson, W.; Eldridge, J.; Glossop, B.; Willmott, G. A Variable Pressure Method for Characterizing Nanoparticle Surface Charge Using Pore Sensors. *Anal. Chem.* **2012**, *84*, 3125–3131.
206. Wang, G.; Zhang, B.; Wayment, J. R.; Harris, J. M.; White, H. S. Electrostatic-Gated Transport in Chemically Modified Glass Nanopore Electrodes. *J. Am. Chem. Soc.* **2006**, *128*, 7679–7686.

207. Wang, G.; Bohaty, A. K.; Zharov, I.; White, H. S. Photon Gated Transport at the Glass Nanopore Electrode. *J. Am. Chem. Soc.* **2006**, *128*, 13553–13558.
208. Shim, J. H.; Kim, J.; Cha, G. S.; Nam, H.; White, R. J.; White, H. S.; Brown, R. B. Glass Nanopore-Based Ion-Selective Electrodes. *Anal. Chem.* **2007**, *79*, 3568–3574.
209. Wang, X.; Smirnov, S. Label-Free DNA Sensor Based on Surface Charge Modulated Ionic Conductance. *ACS Nano* **2009**, *3*, 1004–1010.
210. Takmakov, P.; Vlassiouk, I.; Smirnov, S. Sensing DNA Hybridization *via* Ionic Conductance through a Nanoporous Electrode. *Analyst* **2006**, *131*, 1248–1253.
211. Li, S. J.; Li, J.; Wang, K.; Wang, C.; Xu, J. J.; Chen, H. Y.; Xia, X. H.; Huo, Q. A Nanochannel Array-Based Electrochemical Device for Quantitative Label-Free DNA Analysis. *ACS Nano* **2010**, *4*, 6417–6424.
212. de la Escosura-Muñiz, A.; Merkoçi, A. Nanoparticle Based Enhancement of Electrochemical DNA Hybridization Signal Using Nanoporous Electrodes. *Chem. Commun.* **2010**, *46*, 9007–9009.
213. Lan, W. J.; Holden, D. A.; Zhang, B.; White, H. S. Nanoparticle Transport in Conical-Shaped Nanopores. *Anal. Chem.* **2011**, *83*, 3840–3847.
214. de la Escosura-Muñiz, A.; Merkoçi, A. Label-Free Voltammetric Immunosensor Using a Nanoporous Membrane Based Platform. *Electrochem. Commun.* **2010**, *12*, 859–863.
215. de la Escosura-Muñiz, A.; Merkoçi, A. A Nanochannel/Nanoparticle-Based Filtering and Sensing Platform for Direct Detection of a Cancer Biomarker in Blood. *Small* **2011**, *7*, 675–682.
216. de la Escosura-Muñiz, A.; Chunglok, W.; Surareungchai, W.; Merkoçi, A. Nanochannels for Diagnostic of Thrombin-Related Diseases in Human Blood. *Biosens. Bioelectron.* **2012**, http://dx.doi.org/10.1016/j.bios.2012.05.021.
217. Hou, Y.; Gochin, M. Artificial Ion Channel Biosensor in Human Immunodeficiency Virus gp41 Drug Sensing. *Anal. Chem.* **2008**, *80*, 5924–5929.
218. Matsumoto, F.; Nishio, K.; Masuda, H. Flow-Through Type DNA Array Based on Ideally Ordered Anodic Porous Alumina Aubstrate. *Adv. Mater.* **2004**, *16*, 2105–2108.
219. Ma, C.; Yeung, E. S. Entrapment of Individual DNA Molecules and Nanoparticles in Porous Alumina Membranes. *Anal. Chem.* **2010**, *82*, 654–657.
220. Kim, J.; Voelkerding, K. V.; Gale, B. K. Patterning of a Nanoporous Membrane for Multi-sample DNA Extraction. *J. Micromech. Microeng.* **2006**, *16*, 33–39.
221. McNally, B.; Singer, A.; Yu, Z.; Sun, Y.; Weng, Z.; Meller, A. Optical Recognition of Converted DNA Nucleotides for Single-Molecule DNA Sequencing Using Nanopore Arrays. *Nano Lett.* **2010**, *10*, 2237–2244.
222. Santos, A.; Balderrama, V. S.; Alba, M.; Formentín, P.; Ferré-Borrull, J.; Pallarès, J.; Marsal, L. F. Nanoporous Anodic Alumina Barcodes: Toward Smart Optical Biosensors. *Adv. Mater.* **2012**, *24*, 1050–1054.
223. Lin, V. S. Y.; Motesharei, K.; Dancil, K. S.; Sailor, M. J.; Ghadiri, M. R. A Porous Silicon-Based Optical Interferometric Biosensor. *Science* **1997**, *278*, 840–843.
224. Dancil, K. P. S.; Greiner, D. P.; Sailor, M. J. A Porous Silicon Optical Biosensor: Detection of Reversible Binding of IgG to a Protein A-Modified Surface. *J. Am. Chem. Soc.* **1999**, *121*, 7925–7930.
225. Álvarez, S. D.; Li, C. P.; Chiang, C. E.; Schuller, I. K.; Sailor, M. J. A Label-Free Porous Alumina Interferometric Immunosensor. *ACS Nano* **2009**, *3*, 3301–3307.
226. Lv, X.; Mo, J.; Jiang, T.; Zhong, F.; Jia, Z.; Li, J.; Zhang, F. Novel Multilayered Porous Silicon-Based Immunosensor for Determining Hydroxysafflor Yellow A. *Appl. Surf. Sci.* **2011**, *257*, 1906–1910.
227. DeLouise, L. A.; Kou, P. M.; Miller, B. L. Cross-Correlation of Optical Microcavity Biosensor Response with Immobilized Enzyme Activity. Insights into Biosensor Sensitivity. *Anal. Chem.* **2005**, *77*, 3222–3230.
228. Ouyang, H.; DeLouise, L. A.; Miller, B. L.; Fauchet, P. M. Label-Free Quantitative Detection of Protein Using Macroporous Silicon Photonic Bandgap Biosensors. *Anal. Chem.* **2007**, *79*, 1502–1506.
229. Moretti, L.; Rea, L.; De Stefano, L.; Rendina, I. Periodic *versus* Aperiodic: Enhancing the Sensitivity of Porous Silicon Based Optical Sensors. *Appl. Phys. Lett.* **2007**, *90*, 191112.
230. Bonanno, L. M.; Kwong, T. C.; DeLouise, L. A. Label-Free Porous Silicon Immunosensor for Broad Detection of Opiates in a Blind Clinical Study and Results Comparison to Commercial Analytical Chemistry Techniques. *Anal. Chem.* **2010**, *82*, 9711–9718.